


2011

Feasibility of Wearable Sensors to Determine Gait Parameters

Mario Alves Simoes

University of South Florida, msimoes@tampabay.rr.com

Follow this and additional works at: <http://scholarcommons.usf.edu/etd>

 Part of the [American Studies Commons](#), and the [Biomedical Engineering and Bioengineering Commons](#)

Scholar Commons Citation

Simoes, Mario Alves, "Feasibility of Wearable Sensors to Determine Gait Parameters" (2011). *Graduate Theses and Dissertations*.
<http://scholarcommons.usf.edu/etd/3346>

This Thesis is brought to you for free and open access by the Graduate School at Scholar Commons. It has been accepted for inclusion in Graduate Theses and Dissertations by an authorized administrator of Scholar Commons. For more information, please contact scholarcommons@usf.edu.

Feasibility of Wearable Sensors to Determine Gait Parameters

by

Mario A. Simoes

A thesis submitted in partial fulfillment
of the requirements for the degree of
Master of Science in Mechanical Engineering
Department of Mechanical Engineering
College of Engineering
University of South Florida

Major Professor: Rajiv Dubey, Ph.D.
Stephanie Carey, Ph.D.
Kevin Hufford, M.S.M.E.
Redwan Alqasemi, Ph.D

Date of Approval:
July 7, 2011

Keywords: Stride Length, Cadence, APDM, Vicon, mTBI

Copyright © 2011, Mario A. Simoes

Acknowledgements

This project was funded in part by Draper Laboratory and the University of South Florida. Thanks are given to APDM for providing support for this project in collaboration with Draper Laboratory. In addition, thanks are given to Jamal Saad, Derek Lura and Matt Wernke for their assistance with running the Vicon system and helping program the pipeline in Visual 3D. Thanks are given to Ashley Vincent for assisting in the data processing in Statistical Package for the Social Sciences (SPSS).

Table of Contents

List of Tables	iii
List of Figures	iv
Abstract	vi
Chapter 1 - Introduction	1
1.1 Goal of Thesis	2
Chapter 2 - Background	3
2.1 Mild Traumatic Brain Injury	3
2.2 Timed Up and Go (TUG)	4
2.3 Abnormalities Relative to Mild Traumatic Brain Injury	5
2.3.1 Cadence and Obstacle Avoidance	5
2.3.2 Stride Length	6
2.3.3 Eye, Head and Torso Rate of Rotation	7
2.3.4 Selected Gait Abnormalities Relevant to mTBI	8
2.3.5 Wearable Sensor Technology	8
2.3.6 Accelerometers	9
2.3.7 Piezoresistive Accelerometers	10
2.3.8 Piezoelectric Accelerometers	11
2.3.9 Differential Capacitive Accelerometers	12
2.3.10 Gyroscopes	13
2.3.11 Optical Tracking System	13
2.4 Commercially Available Sensor System	15
2.4.1 AMM Sensor	15
2.4.2 APDM Opal Movement Monitor System	16
2.4.3 InertiaCube BT	17
2.4.4 Zephr BioHarness BT	18
2.4.5 Gait Mat II	18
2.4.6 Vicon System	19
2.5 mTBI System Monitor Selection	20
2.5.1 Equipment Purchased and Utilized	22
Chapter 3 - Methods	25
3.1 Institutional Review Board Approval	25
3.1.1 Volunteer Data	25
3.2 Experimental Setup	26

3.3	Experimental Trials	32
3.4	APDM Configuration	35
3.5	VICON Calibration.....	36
Chapter 4 - Data Analysis.....		38
4.1	APDM Data	38
4.1.1	Cadence.....	39
4.1.2	Torso Rate of Rotation	43
4.1.3	Head Rate of Rotation.....	45
4.1.4	Stride Length.....	48
4.2	VICON Data	54
4.2.1	Cadence.....	55
4.2.2	Torso Rate of Rotation	57
4.2.3	Head Rate of Rotation.....	58
4.2.4	Stride Length.....	60
4.3	Correlation	62
Chapter 5 - Results.....		64
5.1	Cadence Correlation	64
5.1.1	Torso Rate of Rotation Correlation.....	67
5.1.2	Head Rate of Rotation Correlation	69
5.1.3	Stride Length Correlation	71
Chapter 6 - Discussion and Limitations		74
6.1	Discussion.....	74
6.2	Limitations.....	77
Chapter 7 - Conclusion and Future Work		79
7.1	Conclusion	79
7.2	Future Work	80
References		81
Appendices.....		85
Appendix A - Pipeline.....		86
Appendix B - APDM Release Statement.....		97

List of Tables

Table 1: Selection Guide for the Sensor System	21
Table 2: Itemized List of Items Purchased From APDM	23
Table 3: Reflective Marker Locations	30
Table 4: Marker Descriptions.....	31
Table 5: Session and Head Rate of Rotation Speed	34
Table 6: Monitor Labels Locations.....	36
Table 7: Maximum and Minimum Peaks of Head	47
Table 8: Head Rate of Rotation Data.....	60
Table 9: Correlation Values for Pearson's R Correlation	62
Table 10: Average Trials for Cadence	65
Table 11: Cadence Correlation Values.....	66
Table 12: Average Rate of Rotation for the Torso	67
Table 13: Torso Rate of Rotation Correlation Values	68
Table 14: Average Rate of Rotation for Head.....	69
Table 15: Head Rate of Rotation Correlation Values.....	70
Table 16: Average Stride Length.....	71
Table 17: Stride Length Correlation Values.....	72
Table 18: Pearson's R Correlation Values.....	74

List of Figures

Figure 1: Diagram of a Standard Piezoresistive Accelerometer	10
Figure 2: Schematic of a Piezoelectric Accelerometer	11
Figure 3: Diagram of a Differential Capacitive Accelerometer	12
Figure 4: Optical Tracking Cameras Focused on Subject	14
Figure 5: Accessories for APDM.....	22
Figure 6: Collation of Axis on Both Systems.....	23
Figure 7: Configuration of the Docking Station and Access Point.....	24
Figure 8: Configuration of Vicon Cameras for Study	27
Figure 9: Subject in Ready Position.....	28
Figure 10: Monitors and Reflective Markers Mounted on a Subject	29
Figure 11: Static Trial	33
Figure 12: Tab Structure of Mobility Lab.....	35
Figure 13: Calibrated Instruments	37
Figure 14: Trunk Gyroscope Data for Subject	38
Figure 15: Sample Foot Movement [2, 5]	41
Figure 16: Zoom in on Right Leg Data of One Subject Trial	42
Figure 17: Cadence from Mobility Lab.....	43
Figure 18: Yaw Representation on Sternum Monitor.....	44
Figure 19: Peak Turn Velocity in Mobility Lab.....	45
Figure 20: Head Monitor Rotation on Subject.....	46
Figure 21: Filtered Gyroscope Head Data	47

Figure 22: Pendulum Model of Stride Length [13, 26]	50
Figure 23: Stride Length from Mobility Lab.....	54
Figure 24: Right Heel Marker on Vicon.....	56
Figure 25: Left and Right Heel Marker on Vicon Joined	56
Figure 26: Rate of Rotation of the Torso	58
Figure 27: Plane of Markers on Subject's Head	59
Figure 28: Vicon Head Rotation about Central Axis	60
Figure 29: Stride Length of Right Foot.....	62
Figure 30: Correlation Graph of Cadence.....	66
Figure 31: Correlation for Rate of Rotation for Torso.....	68
Figure 32: Correlation for Rate of Rotation of the Head	70
Figure 33: Correlation for Stride Length	72

Abstract

A wearable system that can be used in different settings to collect gait parameters on subjects with a mild traumatic brain injury (mTBI) would allow clinicians to collect needed data of subjects outside of the laboratory setting. Mild traumatic brain injuries stem from a number of causes such as illnesses, strokes, accidents or battlefield traumas. These injuries can cause issues with everyday tasks, such as gait, and are linked with vestibular dysfunction [1]. Different wearable sensor systems were analyzed prior to starting this study along with relevant gait parameters associated with mild traumatic brain injury. To monitor gait parameters relevant to mild traumatic brain injury (cadence, torso rate of rotation, head rate of rotation and stride length) a wearable sensor system was selected (APDM Opal Movement Monitor [13]) and compared against the gold standard optical tracking system (Vicon) [2]. A group of ten, 20-27 year old, healthy subjects were used to validate the APDM Movement Monitor system using the Pearson's R correlation value [35]. Subjects were asked to wear the APDM movement monitors in conjunction with the reflective markers of the Vicon system while performing three sessions of gait trials: a normal gait speed, a fast gait speed and a slow gait speed. Using the Pearson's R correlation values, cadence, torso rate of rotation, and head rate of rotation were found to be highly correlated between both systems. The Pearson's R correlations for cadence,

torso rate of rotation, head rate of rotation and stride length were 0.967, 0.907, 0.942, and 0.861, respectively. These correlation values suggest the gait parameters relevant to mild traumatic brain injury are highly correlated between both the APDM Movement Monitor system and the Vicon system, and APDM's wearable sensor system was lightweight, portable and less costly than the Vicon system.

Chapter 1 - Introduction

The leading causes of traumatic brain injury (TBI) in the US are falls (28%), motor vehicle accidents (20%) and assaults (11%) [3]. Resultant gait abnormalities can include decreased cadence, shorter stride lengths and hesitation while performing a task. TBI can cause a wide range of symptoms depending on the severity of the TBI. There are approximately four categories that TBI effect: motor function, sensory response, cognitive and behavioral dysfunction. Sensory disturbances, spasticity, decreased coordination and motor control issues are all signs of motor deficits in TBI patients [4]. Patients suffering from mild to severe TBI may require some form of assistance in rehabilitation from a clinician.

A device that can monitor subjects at home can potentially assist in a faster rehabilitation [5]. A cost effective wearable sensor system, that has the same reliability as the gold standard of an optical tracking system, would aid in the rehabilitation of subjects with a mild traumatic brain injury. A device that would be less intrusive to the subject and can be worn outside the Laboratory would provide better representation of the individual's abnormalities. This device should be a commercially available system that can be used to monitor parameters associated with a mild traumatic brain injury (mTBI).

Wearable sensor systems are devices that contain small sensors such as inertial measurement units that can be worn on the body. An inertial measurement unit contains a triaxial accelerometer, triaxial gyroscope and triaxial magnetometer. The system can utilize some form of the inertial measurement unit or use the entire unit. Software packages are used to read these sensors and provide feedback to the user on what the system measures. Typically, these systems are validated against gold standard systems which are considered to be the best known systems available to perform the desired operation [6], such as an optical tracking system [2]. An optical tracking system utilizes optical tracking cameras that track the movement of subjects performing various tests while wearing precisely located markers that represent body segments.

1.1 Goal of Thesis

The primary goal of this study was to determine the feasibility of a commercially available wearable sensor system against an optical tracking system that is considered to be the gold standard. A wearable sensor system must be able to accurately monitor gait parameters relevant to mild traumatic brain injury which are: cadence, torso rate of rotation, head rate of rotation, and stride length.

Chapter 2 - Background

2.1 Mild Traumatic Brain Injury

Traumatic brain injuries can stem from a number of causes such as illnesses, strokes, accidents, and battlefield traumas. These traumas, depending on the severity, can cause a brain injury. Symptoms of an mTBI can cause an individual to have issues performing everyday tasks [1, 7]. Damage to the vestibular system can cause subjects to lose the ability to maintain balance during a normal task. Walking and vision are normal tasks that depend on the vestibular system, and when damaged, these tasks become extremely difficult to maintain [8]. Subjects compensate by slowing down and hesitating while performing a task. As an example, subjects with gait disorders from an mTBI can lack the confidence to walk normally. A normal subject would take a stride length of approximately 1.5 meters, while an individual with an mTBI would take a 1.2 meter stride length because of the lack of confidence to judge the distance [9, 10]. These variations in subject's tasks can be picked up using clinical evaluation tools [11].

Clinicians use these evaluation tools to help them assess a patient's disorder: two common types of tests are Berg Balance Scale (BBS) and Dynamic Gait Index (DGI). The BBS tests are strictly used to monitor the balance of a patient with vestibular disorders. A scale from 0 to 4 (0 indicates the lowest

performance while 4 indicates the highest attainable) used to rate the performance of the individual on 14 functional mobility items. While the BBS test was designed to test balance, gait abnormalities are best assessed using the DGI, which rates a participant from 0 to 3 (0 being the lowest and 3 being the highest attainable score) on 8 commonly occurring tasks [11]. These tasks include normal walking, walking at different speeds, walking with head turned, walking and turning, walking around and over obstacles and stair climbing.

2.2 Timed Up and Go (TUG)

A timed up and go test was designed to measure vestibular dysfunction. This test requires subjects to sit with their back to a chair and then they would get up and walk 10ft (3m), then turn around and come back to the chair. Once at the chair, they would rotate and sit down. Subjects were given multiple trials so as to average the trial times. The duration of the test in seconds is used to rate each individual as follows:

- If the task is completed in less than 10 seconds, the individual is generally freely mobile.
- If the task is completed in 10-20 seconds, the individual is mostly independent.
- If the task is completed in 20-29 seconds, the individual has variable mobility.
- If the task is completed in more than 29 seconds, the individual is mobility impaired [5, 12, 13].

2.3 Abnormalities Relative to Mild Traumatic Brain Injury

Subjects with an mTBI exhibit symptoms differently depending on the severity of the brain injury. Issues with the vestibular system contribute to the inability of an individual to balance themselves. The body's vestibular system allows the body to control its balance or recognize its sense of spatial orientation. Disorders of this type are induced by blast, illness, and physical trauma to the brain [1, 4, 7, 14]. Since there are so many abnormalities that a subject can exhibit, determining which parameters were most relevant to a majority of mTBI subjects was part of this study.

2.3.1 Cadence and Obstacle Avoidance

Cadence is the amount of steps per minute and is unique to every individual. Normal gait in most mTBI studies are determined by sampling a population of healthy individuals and using this data as normative data [10, 16]. A subject in question would either exhibit below the normal or above the normal dependent on the severity of the symptoms. As normal subjects walk, they have confidence present in their gait and a sense of competency due to years of walking [10]. Individuals with an mTBI would have a reduced cadence as compared to normal subjects [15]. Clinicians would test a subject along a defined path and time the trial. Subjects that exhibit symptoms will generally have slower speeds as compared to normative data. Reduced cadence is present in almost all types of mTBI and the degree of severity is dependent on the injury. In general, cadence decreases in most mTBI cases [1, 7, 14, 15].

Obstacle avoidance can be affected by a subject's inability to judge the obstacle or by lacking the confidence to perform the avoidance. Obstacle avoidance is an everyday task that is constantly overlooked. These obstacles may include uneven streets, holes, and pieces of debris blocking a path [15]. Normal individuals develop habitual tendencies and underestimate the actual process of avoiding obstacles, becoming second nature. Subjects lacking the ability to overcome an obstacle, such as walking over it, could fall because of instability. Subjects lacking the confidence to perform the task believe that if a certain step is taken, it will cause them to fall or become unstable. As a result, subjects would make compromises in gait in order to successfully avoid the obstacle or overcome it. This abnormality is tested using the Dynamic Gait Index which adds a gap of some distance that a patient must overcome and they are scored on a scale based on the performance [11, 16].

2.3.2 **Stride Length**

Stride length is the distance between consecutive heel strikes of the same foot. Subjects with an mTBI exhibit a smaller stride length as compared to a healthy subject of the same body type. The stride length in each mTBI case is different depending on the severity of the injury, but this abnormality is present in all mTBI cases [4, 7, 10, 18]. The reduction in stride lengths is caused by the vestibular system being damaged. With the vestibular system being damaged, subjects could become unstable and increase the risk of fall. As a result, subjects

would become hesitant in taking a bigger stride and end up decreasing their stride length to minimize the risk of fall or destabilization [1, 4].

2.3.3 Eye, Head and Torso Rate of Rotation

The vestibular system sends control signals to the neural structures that control the eye and this system is composed of sensory inputs from the eyes and inner ear. The eyes will move relevant to the head movement and as the head turns in one direction, the eyes will turn in the opposite direction keeping track of the object in view. This process is called the vestibulo-ocular reflex, and uses the eyes and inner ear to control the stability of the body in a type of control system environment [16]. Any interruption in this control system could affect the function of the vestibular system which would cause the body to become unstable. When the eyes lose track of the object they are on, they present the mTBI subject with unwanted symptoms such as: dizziness, confusion, headaches and inability to balance while moving [17]. A prime example of this is when subjects are asked to track a wall mounted clock while moving forward. As they walk, they shift their head from left to right while keeping their eyes on the clock. If subjects with an mTBI rotate their head, their eyes may lose track of the object they were looking at.

In conjunction with eye motion, the rate of rotation of the head and torso also play roles in gait. The eyes and the head work in conjunction to monitor balance and control using the vestibular system located in the head. When the torso performs a turn, it causes the head (which houses the vestibular system) to rotate in respect to the torso. Clinical evidence suggests that patients with mTBI

having a head and torso rate of rotation greater than 85-100 degrees per second would tend to exhibit vestibular dysfunction [18]. This would cause subject's fall risk to increase. The rates of rotations are pertinent to torso as well as the head and eyes because the torso drives the rotation of the head during turns. Current studies are being done at clinical labs to monitor eye, head and torso rates of rotation. Clinical evidence suggests that eye, head and torso rates of rotation are prime indicators of the severity of an mTBI. Most subjects that have an mTBI have damage done to their vestibular system [7, 18]. A rate of rotation past the 85-100 degrees per second would cause the subject to become disoriented and increase their risk of a falling [18].

2.3.4 Selected Gait Abnormalities Relevant to mTBI

The selected gait parameters for this study are present in all mTBI cases: cadence, torso rate of rotation, head rate of rotation and stride length. The parameters selected were all different from one another and were used in this study to validate a wearable sensor system. Studies were conducted using groups of these parameters together in one form or another to test subjects with mild to severe TBI. [7].

2.3.5 Wearable Sensor Technology

Wearable sensors are used in academic settings for many studies. Universities and organizations have come up with different iterations of wearable sensor systems. While academia produces new technology quickly, this technology does not enter the commercial market as quickly, and it is often not

commercially available [19]. Determining which system is commercially available and can be used to monitor gait parameters is a part of this study.

Wearable sensor systems typically are composed of inertial measurement units (IMU). IMU's are devices that have accelerometers, gyroscopes and magnetometers all integrated into a single device. The axes of the sensors (Accelerometer, gyroscope and magnetometer) were aligned with one another, while the axes of each sensor were orthogonal to one another. Each wearable sensor system monitors different parameters based on how the system is integrated and designed. The sensors that make up these systems each have a purpose and are explained in detail later on. This study looked for a system that is commercially available, portable, cost efficient and capable of monitoring the following parameters: cadence, torso rate of rotation, head rate of rotation and stride length. The system is required to cost less than a gold standard system such as an optical tracking system. Listed below are types of sensors used within a system, along with what each type of sensor does, and each served a unique purpose within that system.

2.3.6 Accelerometers

Accelerometers are sensors that pick up changes in acceleration. Accelerometers are based on a mechanical sensing unit which consists of a test mass attached to a mechanical suspension system with respect to a reference frame. Inertial forces cause the mass to deflect according to Newton's second law. Accelerations are measured electrically from the impact of the test mass

with respect to the reference frame. Most accelerometers are grouped into three categories: piezoresistive, piezoelectric and differential capacitive accelerometers. Each of these types of accelerometers is used for a specific purpose based on the design of the device [17].

2.3.7 Piezoresistive Accelerometers

Piezoresistive accelerometer units have cantilever beams composed of a special material, such as a crystal, with a test mass on the end [20]. The base portions of the cantilevered beam have strain gauges set in the form of a Wheatstone bridge located around it and are an integral part of the mass as seen in Figure 1. A Wheatstone bridge is an electrical circuit used to measure unknown electrical resistance, which is ideal for measuring strain.

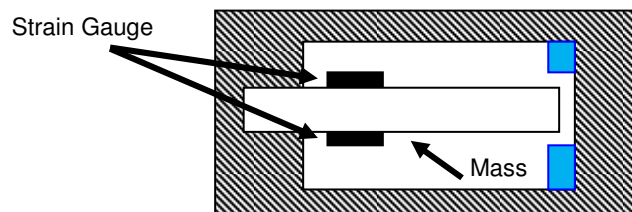


Figure 1: Diagram of a Standard Piezoresistive Accelerometer

When voltage is sent through a Wheatstone bridge, as the cantilevered beam moves, the resistance changes in respect to the acceleration, causing an electrical resistance to be produced and measured. This change in voltage from the strain gauge is picked up using a data acquisition board and processed using a signal processing system. There is a pitfall to this type of sensor, in that it is susceptible to drifts due to temperature variations and/or input voltage irregularities [21, 22]. For example, as data from this accelerometer is recorded

over a period of time, the signal can slowly increase or decrease due to the drifts mentioned. To eliminate these drifts, a filter must be used [13].

2.3.8 Piezoelectric Accelerometers

Piezoelectric accelerometers are units that have a mass supported by a spring-like fixture over a piezo crystal [23]. The components of the device are sealed in a housing unit that is mounted to the object in question. These types of accelerometers are typically used to measure vibrations, and a schematic of this device can be seen in Figure 2. As vibration occurs, the mass vibrates to the frequency of the device and this mechanical motion is then converted to electrical signals and sent to a data acquisition board [22].

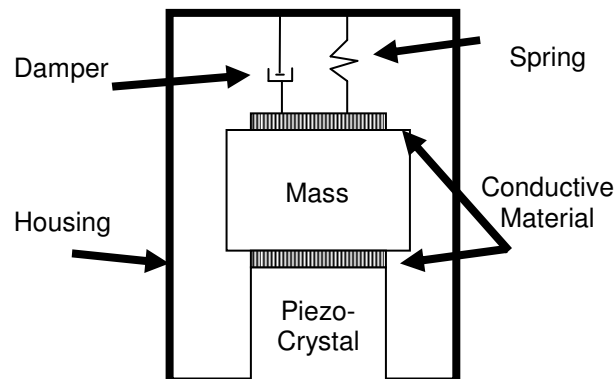


Figure 2: Schematic of a Piezoelectric Accelerometer

These types of sensors have thresholds as to how much vibration they can withstand, and they can have a dynamic range for the sensor which causes it to peak out once it exceeds a certain threshold. The damper cuts down the intensity of the vibration. With all the components integrated together, these

types of accelerometers are ideal for measuring the vibration in mechanical device.

2.3.9 Differential Capacitive Accelerometers

Differential capacitive accelerometers are the most common type of accelerometers available and they are integrated into many devices due to their small size. This system works by using a seismic mass supported between two electrode plates. Conductive material must be used in order to register a capacitance between the electrodes. As motion is applied, the mass moves towards one of the electrodes seen in Figure 3. The capacity difference between the electrodes indicates the direction and intensity of the acceleration. The design of the accelerometer would determine if it is a single axis unit or multi axis unit [3]. The triaxial unit allows for representation of an object by all three axes.

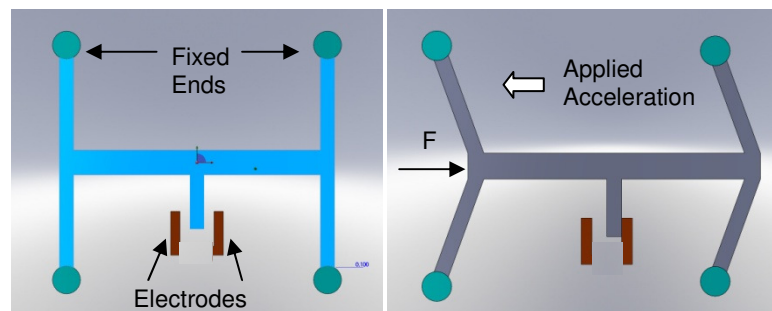


Figure 3: Diagram of a Differential Capacitive Accelerometer

Differential capacitive accelerometers have significantly reduced power consumption and provide faster response compared to piezoresistive and piezoelectric accelerometers [3, 21, 24, 25]. This accelerometer has the

capability of being compact, cost effective, and capable of being microelectromechanical systems (M.E.M.S.) sizes.

2.3.10 Gyroscopes

Gyroscopes are devices used to measure the rotation about an axis in question. A single axis gyroscope measures the rotation of a single axis while a three axis gyroscope measures three different axes. These sensors can be very accurate in controlled conditions. Gyroscopes combined with accelerometers, can be combined together to measure rotational velocities and inertial forces. Gyroscopes can be manufactured in M.E.M.S. scale and used in many devices [13, 26, 27].

The accuracy of a gyroscope typically degrades over time due to drift. Drift occurs when data begins to skew in the positive or negative direction; this can be brought on by temperature changes in the device. In addition, voltage fluctuations can generate drift. Filtering the results can help remove drift from the system [5, 13]. By controlling the drift, the gyroscope can be used as an accurate device for measuring the angular velocity about an axis.

2.3.11 Optical Tracking System

Optical tracking systems utilize camera-based technology to measure precise and accurate movements of a subject. Because of these systems accuracy, they are considered to be a gold standard. The entire system requires the use of a large room to set up the cameras, cables, computer workstations

and calibration equipment. Cameras are placed strategically around an area to provide a field of view that the subject will be working in. Cameras track the markers placed on the subject's body and locations of the markers are dependent on the type of study being conducted. Active markers or passive markers are utilized depending on the study.

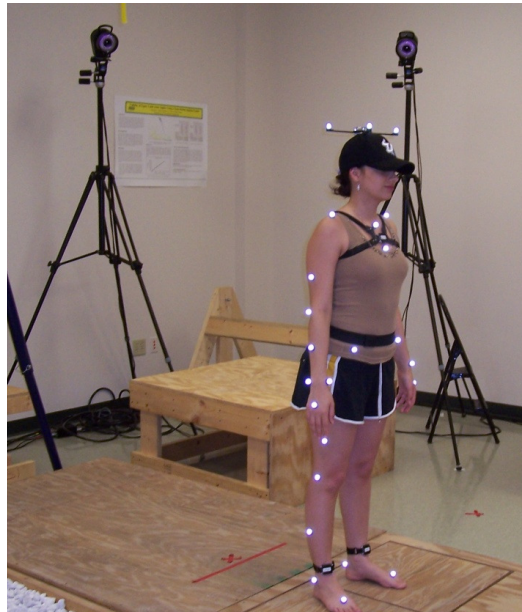


Figure 4: Optical Tracking Cameras Focused on Subject

Passive markers are retro-reflective spherical balls with adhesive backings to them. The markers are wrapped in reflective tape that is highly reflective to infrared illuminators that surround the optical cameras. Figure 4 shows a subject with passive markers and the locations of the optical cameras [28, 29].

Active markers emit light that are picked up by a camera. Markers are spherical in shape and come in different sizes depending on the application required. These markers require hardware and battery power to emit the light

source. Both active and passive markers represent body segments that cameras can track [17].

2.4 Commercially Available Sensor System

Currently, there are commercially available sensor systems that can measure a wide variety of parameters. Listed below are a small handful of systems that can be purchased and utilized for this study. The system must be able to monitor cadence, torso rate of rotation, head rate of rotation and stride length. The system must have the following features:

1. The sensor system components must not weigh more than a standard metal wrist watch.
2. The system must be able to transmit data wirelessly to a computer and store it.
3. The sensor system must have manufacturer's mounting hardware provided, such as straps and harnesses (wearable).
4. Battery life must be no less than 8 hours of continuous use.
5. The system must cost less than a gold standard system.

2.4.1 AMM Sensor

AMM stands for Advanced Motion Measurement, Inc. This company provides a sensor system called AmmSensor, which incorporates a triaxial accelerometer, a triaxial gyroscope and a triaxial magnetometer. These set of sensors are known as an inertial measurement units and are portable units that

can be attached to the body with wrist straps or a harness. The straps and harness are accessories offered by the manufacture for additional purchase. The unit is a rechargeable system that runs approximately 6 hours. The device has a built in auditory feedback speaker that can be programmed to provide feedback to the user. Software must be purchased as a necessity for this product. The system uses one module, and the module can be applied to any area in question. This system did not have a software package to monitor all the parameters desired in this study. The AMM unit cost \$1200.00 and the entire system with the software development kit was \$1895.00.

2.4.2 APDM Opal Movement Monitor System

APDM stands for Ambulatory Parkinson's Disease Monitoring. This company specializes in a product to monitor subjects' gait patterns. This sensor suite was designed for monitoring patients with Parkinson's disease but can be used for monitoring gait parameters relevant to other disorders. These monitor units are called Opal Movement Monitors. In conjunction with the monitor system, a software package called Mobility Lab can be purchased, which records and analyzes the data from the monitors. Mobility Lab has the capability of processing eight movement monitors wirelessly with an access point. The monitors are designed with a triaxial accelerometer, triaxial gyroscope and triaxial magnetometer. The monitors are portable, lightweight and small due to their compact electronics and M.E.M.S technology. The manufacturer had also

created harnesses for the different body locations that the monitor would be placed.

Mobility Lab is known as a host program that configures and runs trials based on plug-ins. The plug-in iTug has the ability to work with Mobility Lab, which requires the subject to perform a modified “timed up and go” test to measure gait parameters. The host software analyzes the data from all the monitors based on the iTug algorithm. Upon completion of the analysis, Mobility Lab displays the data in a full report detailing all the trials and parameters tested [13]. The APDM Opal movement monitor costs \$2399.00 a piece and the entire system, including Mobility Lab, costs \$20,032.00.

2.4.3 **InertiaCube BT**

The InertiaCube BT sensor is a dynamic wireless inertial orientation sensor provided by InterSense Inc. The device has a three-axis gyroscope and has an eight hour battery life. Up to five units can be combined together on the body, and can be strapped on to the body at any desired location. By allowing the user to mount the unit anywhere on the body, a detailed analysis of the desired body segment would be accomplished. This device doesn't have a software package that has the capability of monitoring the gait parameters needed for subjects with vestibular disorders. Applications of this product can be measurements for sports biomechanics, physical therapy and rehabilitation. The device can be used to measure gait patterns and be used to measure rate of rotations of the head and torso. The system does not come with software and

must be created using the software development kit that is purchased from the company. The cost of the InertiaCube BT could not be obtained for this study.

2.4.4 Zephr BioHarness BT

The Zephr BioHarness Bt made by Zephyr is a single module sensor system that is strapped around the sternum. Sensors are sewn into the fabric strap that is wrapped around the subject's sternum. The sensors sewn into the strap measure vitals such as: heart rate, breathing rate and skin temperature. The device is also capable of measuring acceleration, position, and skin conductance at the sternum. The system is compact and has the ability to communicate via Bluetooth to a computer. Incorporated within this device is a triaxial accelerometer. Some of the features that this device also have is its ability to record heart rate, breathing rate, skin temperature, position, skin conductance, ECG logging and 570 hours of data storage. The device only has one unit and cannot monitor gait parameters properly. The primary use of this system is to measure subject's vitals during a trial. The BioHarness costs \$1399.00 and the software development kit is \$849.00 more.

2.4.5 Gait Mat II

The Gait Mat II measures gait parameters from a pressure sensitive mat, which houses embedded pressure switches within the mat itself. The device measures step length, stride length, support base, step time, swing time, stance time, single support time, double support time and average velocity. There are no

sensors that the subject has to wear, which makes this device non-intrusive to the subject. The main inputs for this device are from the user's heel and toe, which drive the calculations in this device. Pressure sensitive switches are equally spaced within the mat. This allows the software to know the exact distance relative to a surrounding sensor. This device measures gait parameters required for the study but does not measure rotation information. The selection requirement that this device does not meet is that it is not portable and wearable outside the laboratory. This system is widely used as a clinical evaluation tool to measure gait parameters. The Gait Mat II costs \$18000.00 and comes with the software to run the device and analyze the data.

2.4.6 **Vicon System**

A Vicon system is an optical tracking system for motion analysis. The system uses multiple optical tracking cameras to monitor human movement. The system calibrates all the cameras to a common reference plane. The type of study drives the configuration for the cameras. This reference plane calibrates to a global coordinate frame, which is referenced in Visual 3D. This plane calibrates the distance between markers for future calculations in the analysis program. The system converts pixels to millimeters and calculates what the distances are based on triangulation. Triangulation is done by taking the 2D image data from two cameras and locating the marker of interest in space to the global coordinate frame. One camera view would provide the x and y coordinate from its own reference plane, while the 2nd camera would provide the x and y coordinate from

its own reference plane as well, and the point at which both image data meet in respect to the global coordinate frame provides the location of the marker in space. This would locate the marker in 3D space providing it with an x, y and z coordinates. The system has an accuracy of 0.5 mm and a sampling rate of 120 Hz [6, 30]. Accuracy in the Vicon system is dependent on the locations of the passive markers on the subject. The markers are placed at key locations on the body that represent a segment on the subject's body. By performing this task on every segment, the subject's physical attributes are represented and are not assumed to be symmetrical. The optical tracking systems, such as the Vicon, are considered the gold standard of gait analysis due to their precision and accuracy [6, 31].

The set up for the system requires a large laboratory to set up the cameras and gait path. A powerful computer is needed to process the data from the Vicon and analyze it. Software packages, such as Visual 3D, are used to analyze the data from trials and in large sets. Visual 3D has the capability of being customizable to the study and can calculate any parameter desired. This system is capable of measuring cadence, torso rate of rotation, head rate or rotation and stride length by using the Visual 3D software. The Vicon system itself costs roughly \$154,000.00 and Visual 3D is \$20,615.00.

2.5 mTBI System Monitor Selection

Three wearable sensor systems, the AMM sensor, APDM system, and InertiCube BT system, were chosen as possible candidates for use in this study,

and all were capable of measuring the desired parameters via the hardware and modified software. The desired gait parameters are: cadence, torso rate of rotation, head rate of rotation and stride length. The sensors were capable of measuring the desired parameters, but the software packages had to be developed. A selection matrix was used to differentiate the systems against one another. The matrix was used to select the best system to be used in this study and the results are broken up into Table1.

The parameters of the matrix were divided up and given factors of importance depending on the scope of the study. The number of sensors per system was critical in developing a system that was accurate and precise.

Table 1: Selection Guide for the Sensor System

	Battery Life (H)	Wireless Connectivity	Latency Recovery	Sensor Type	SDK	Cost per Unit	Storage (Gb)	Number of Sensors per system	Weight (g)	Score
Importance Factor	1	2	1	1	2	1	2	3	2	
AMM	8	✓		IMU	✓	\$1,200.00	0	1	42	10
APDM Opal	16	✓	✓	IMU	✓	\$2,399.00	16	8	22	14
InertiaCube BT	6	✓		Gyroscope	✓	N/A	0	7	67	9

After considerations of all the commercially available systems and what each measured, the best system selected for the given parameters was the APDM system. For the following reasons, APDM's Opal movement monitor and Mobility Lab allowed for optimal calculation of the given parameters:

1. The monitors weigh less than a standard metal wrist watch.
2. The system transmits data wirelessly via ZigBee.
3. Convenient mounting hardware is available from the manufacture.
4. Has a battery life of 16 hours.
5. The system costs less than a gold standard system.
6. The software calculates cadence, torso rate of rotation, head rate of rotation and stride length.

2.5.1 Equipment Purchased and Utilized

The hardware was purchased from APDM and consisted of five Opal movement monitors and Mobility Lab software. With this purchase, the monitors came with the docking stations, chargers, wireless access point, and necessary wiring. Mobility Lab was purchased as beta software that would be used in this study.



Figure 5: Accessories for APDM

Figure 5 shows the accessories purchased from APDM. In order from left to right are a sternum strap, wireless access point, an ankle strap and a waist strap. Table 2 has an itemized list of all the items purchased from APDM. The hat was an item that was custom made to fit the monitor and Vicon markers. The

Vicon markers and Opal monitor were coplanar with one another and both planes had collinear axes as seen in Figure 6. This was a critical design parameter to prevent the need of more complex calculations.

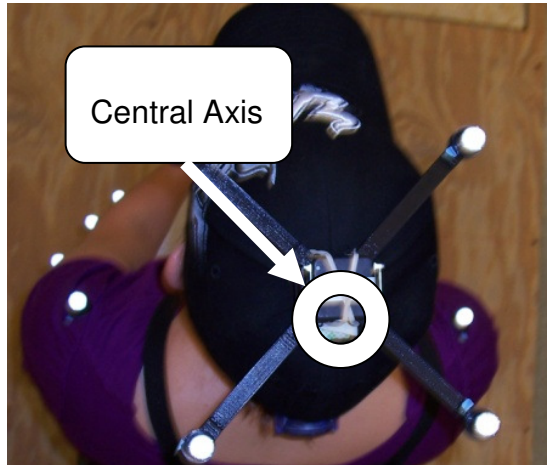


Figure 6: Collation of Axis on Both Systems

For this study the Vicon system was at the University of South Florida's Rehabilitation Robotics Testbed (RRT) facility and was used at this facility. The Vicon system was set up and functional within this facility when this study started. This system utilized eight optical tracking cameras and a custom walkway for gait trials as seen in Figure 4.

Table 2: Itemized List of Items Purchased From APDM

Item	Quantity
Opal Movement Monitor	5
Docking Station	5
Wireless Access Point	1
Sternum Strap	1
Waist Strap	1
Ankle Straps	2
Hat (custom)	1
Mobility Lab & iTug	1

All the cameras were connected to an interface unit that was connected to a computer. The computer was used to gather all the trial data and process it using Visual 3D. Reflective markers used for this study were also purchased to accompany the Vicon system. These markers were to be attached on the subject using a double sided tape and the custom head rig. As part of the head rig, a metronome was purchased to help guide the subject's head shifting from left to right and was clipped onto the back of the hat. The metronome is a programmable tempo timer that has the capability of generating a tone at different intervals of time. The set up of the APDM station is seen in Figure 7 and the Vicon system set up is seen in Figure 8 in the following chapter.



Figure 7: Configuration of the Docking Station and Access Point

Chapter 3 - Methods

This study examined the feasibility of using APDM's Opal movement monitors to detect selected gait parameters: cadence, torso rate of rotation, head rate of rotation and stride length against the gold standard of the Vicon system.

3.1 Institutional Review Board Approval

This study was approved by the institutional review board at the University of South Florida (IRB: Pro00003205) as a minimal risk study. The study was conducted at the University of South Florida's RRT facility and complied with all institutional review board protocols.

3.1.1 Volunteer Data

The IRB protocol stated that individuals between the ages of 18 and 65 were eligible for this study. A total of ten subjects were required to complete this study. This study selected five men and five women between the ages of 20 and 27. Selection criteria required the subjects to be healthy and free of any gait abnormalities. Subjects selected for this study volunteered to participate.

Subjects who participated in this study signed a consent form allowing for the physical measurement of their body to be recorded, as well as participation in this study. By signing the consent form, it signified that the subject understood

the study and the potential risks. Subjects were given a unique identification number to protect their privacy. Data relating the subject to their id code was locked away from public view and only study personnel were allowed to review this data.

3.2 Experimental Setup

The study took place at the University of South Florida's RRT facility that housed the Vicon system, along with a lab space of 20'x 30' with an eight-meter-long wooden walkway. The walkway was the path on which subjects walked for each trial, and was located in the middle of eight optical tracking cameras mounted on adjustable tripods as seen in Figure 8. The field of view of the Vicon system was not able to monitor the full seven-meter walkway required for this study. The cameras were instead focused on the end of the walkway where the subject turned, allowing for optimal data collection at this location during each trial. The field of view was limited and allowed a limited space to collect data. The Vicon system required at least one full gait cycle to gather gait data, but in this study, the camera system monitored four gait cycles of the subject. Once all the cameras were located, the cameras were connected to a central station (computer) which powered and received the data. The Vicon system was calibrated to ensure accurate readings for each subject and recalibration was repeated before each subject.

In contrast to the Vicon system, the APDM system was able to record the entire walkway on its monitors and did not require any modifications. This system

required at least three full stride lengths (roughly 7 meters) in order to calculate the needed gait parameters. The APDM system required the least set up in terms of hardware and space, and only needed a standard table that supported the laptop, docking stations, and wireless access point (Figure 7). Both systems needed to pick up cadence, torso rate of rotation, head rate of rotation and stride length.



Figure 8: Configuration of Vicon Cameras for Study

The set up was designed to optimally record data from both sets of systems simultaneously. A chair was placed at the start of the seven meters as seen in Figure 8, and a mark was placed at the seven meter line to signal the subject to turn around. This test was a modified timed up and go test, iTug. Figure 9 shows the subject in the ready position sitting in a chair prior to the trial. Subjects started the trial and walked into the field of view of the Vicon and then walked back to get back to the chair. Monitors and markers were placed on the

subject prior to each set of trials. APDM monitors were placed at key locations specified by APDM, which are the sternum, lower lumbar, lower shank and head as seen in Figure 9.



Figure 9: Subject in Ready Position

Hardware used to mount the Opal monitors was adjusted for each individual to ensure that the monitors were secure. The monitors were placed on the subject first before the reflective markers of the Vicon system. A custom rig was developed and used to hold the head monitor and four reflective markers about the subject's central axis on the head. This rig was sewn onto the top of

the hat seen in Figure 10. The hat used was a one size fits all, which was worn on the top of the head along with a metronome that was clipped on the back side of the hat. The metronome was used only during the fast and slow trials.

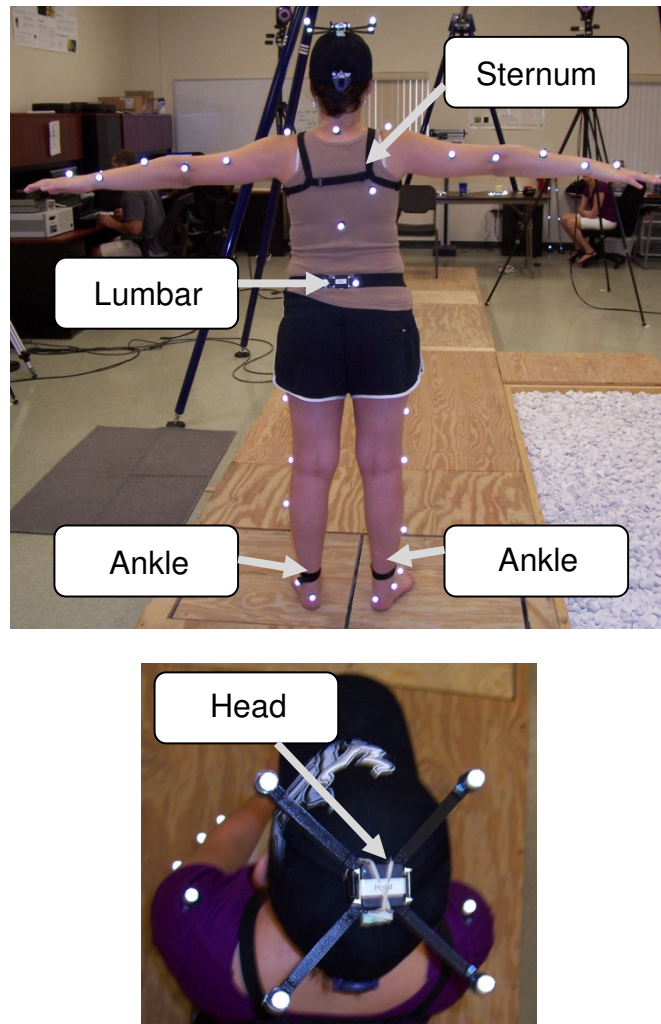


Figure 10: Monitors and Reflective Markers Mounted on a Subject

Once all the monitors were properly secured on the body, the reflective markers were attached to the subject. Using a checklist to assist in properly placing the markers was essential for consistency for each subject. The markers

were placed on key locations, such as the joints, to accurately represent segments of the body. Table 3 lists all the locations that require a reflective marker and are represented in Figure 10.

Table 3: Reflective Marker Locations

Torso	Right Leg	Left leg	Waist	Right Arm	Left Arm
<input type="checkbox"/> RSHO	<input type="checkbox"/> RTHI	<input type="checkbox"/> LTHI	<input type="checkbox"/> RASI	<input type="checkbox"/> RUPA	<input type="checkbox"/> LUPA
<input type="checkbox"/> LSHO	<input type="checkbox"/> RKNE	<input type="checkbox"/> LKNE	<input type="checkbox"/> LASI	<input type="checkbox"/> RELB	<input type="checkbox"/> LELB
<input type="checkbox"/> CLAV	<input type="checkbox"/> RTIB	<input type="checkbox"/> LTIB	<input type="checkbox"/> RPSI	<input type="checkbox"/> RWRA	<input type="checkbox"/> LWRA
<input type="checkbox"/> STRN	<input type="checkbox"/> RANK	<input type="checkbox"/> LANK	<input type="checkbox"/> LPSI	<input type="checkbox"/> RWRB	<input type="checkbox"/> LWRB
<input type="checkbox"/> RBAK	<input type="checkbox"/> RTOE	<input type="checkbox"/> LTOE	Head	<input type="checkbox"/> RFIN	<input type="checkbox"/> LFIN
<input type="checkbox"/> T10	<input type="checkbox"/> RHEE	<input type="checkbox"/> LHEE	<input type="checkbox"/> Wear Hat	<input type="checkbox"/> RFRA	<input type="checkbox"/> LFRA
<input type="checkbox"/> C7					

Markers were placed according to the descriptions listed in Table 4. This configuration allowed accurate representation of the body's movement during the trials. The marker placements were consistent between subjects. The head markers were mounted on a fixture coplanar with an APDM monitor on a standard baseball hat; this kept the center of rotation consistent between the two systems.

Table 4: Marker Descriptions

Code name	Marker description	Marker placement
C7	7th Cervical vertebrae	Spinous process of the 7th cervical vertebrae
T10	10th Thoracic vertebrae	Spinous process of the 10th thoracic vertebrae
CLAV	Clavicle	Jugular notch where the clavicles meet the sternum
STRN	Sternum	Xiphoid process of the sternum
RBAK & LBAK	Right & Left back	Middle of the right scapula (asymmetrical)
RSHO & LSHO	Right & Left shoulder	Right acromio-clavicular joint
RUPA & LUPA	Right & Left upper arm	Placed on the upper arm between the elbow and shoulder markers
RELB & LELB	Right & Left elbow	Right lateral epicondyle approximating elbow joint axis
RWRA & LWRA	Right & Left wrist A	Wrist thumb side
RWRB & LWRB	Right & Left wrist B	Wrist pinkie side – on the pisiform
RFIN & LFIN	Right & Left finger	On the dorsum of the hand just below the head of the right third metacarpal
RFRA & LFRA	Right & Left forearm	Placed on the lower arm between the wrist and elbow markers
RTHI & LTHI	Right & Left thigh	Place the marker over the lower lateral 1/3 surface of the thigh
RKNE & LKNE	Right & Left knee	Placed on the lateral epicondyle of the left knee
RTIB & LTIB	Right & Left tibia	Placed on the lower 1/3 of the shank
RANK & LANK	Right & Left ankle	Placed on the lateral malleolous
RTOE & LTOE	Right & Left toe	Placed of the second metatarsal head
RHEE & LHEE	Right & Left heel	Placed on the calcaneous
RASI & LASI	Right & Left Asis	Placed directly over the anterior superior iliac spine
RPSI & LPSI	Right & Left PSIS	Placed directly over the posterior superior iliac spine

The Vicon system needed to be calibrated properly and this was done after the subject was prepped to aid in maximizing the accuracy and precision. Calibration allowed for accurate segment lengths between markers. The Vicon system required at least two markers to create a segment and three markers to create a plane. Segments were set up properly according to Table 4. The torso rate of rotation and head rate of rotation required a plane to accurately measure the rate of rotation of those segments. Body segments composed of planes, such as the torso and head, were groups of at least three markers that came together to form a plane. Creating these planes was essential in computing the gait parameters in Visual 3D.

3.3 Experimental Trials

Subjects performed three types of sessions with three trials within each session. All sessions were performed a modified TUG test, which required the distance of the path to be extended from three meters to seven meters. The procedure for perform the test was the same as the traditional TUG test. Trials started when the subjects were instructed to walk. Subjects stood up and walked to a mark on the floor. At the mark, they rotated 180 degrees to their left, and came back to the chair, where they rotated 180 degrees in the same direction to sit. Testing required two operators, one that operated the Vicon system and the other that operated the APDM system. The synchronization between the systems was done using verbal communication. The operator of the APDM signaled the

Vicon operator signifying the start of both systems. The trial ended when the APDM operator signaled for a stop.

Each subject also performed a static trial which required the subject to stand straight up with their arms straight out as Figure 11 shows. This process allowed for the auto labeling of the markers using Table 4 in the Vicon workstation, which simplified the model generation process.



Figure 11: Static Trial

The first session that subjects performed was a normal gait speed in which a subject walked a normal gait speed with normal head movement. The subject repeated this three times.

The next session was the fast walk, in which subjects increased their gait speed faster than their normal, and shifted their head side to side with the help of a metronome. The metronome was used as a guide to help assist the subject to know where their head should be and at what repetition. The metronome was set to 0.94 seconds a beat which resembled a higher rate (100 degrees per second) of rotation than an mTBI threshold of 85 degrees per second [18]. This threshold was the rate at which an mTBI subject would not lose vestibular function. Subjects were given two test trials to acclimate themselves to the session.

The third session was the slow walk, where the subject decreased their gait speed slower than their normal speed, and shifted their head slower. The metronome was set to the mTBI threshold of 85 degrees per second which was 0.74 seconds per beat. Once again subjects were given two test trials to acclimate themselves to the metronome and slower speeds. Table 5 shows all the session information used for this study.

Table 5: Session and Head Rate of Rotation Speed

Session	Trials	Metronome	Walking Speed
Normal Walk	3	N/A	Normal Speed
Fast Walk	3	0.94 sec /beat	Faster than Normal
Slow Walk	3	0.74 sec/beat	Slower than Normal

3.4 APDM Configuration

The APDM system was configured once prior to testing the subjects. The configuration process labeled the locations of the monitors, to the monitors themselves in the software. This allowed the software to differentiate the monitors from one another and use the correct data.

Monitors were given specific identification numbers from the manufacturer that was unique to the monitors and the wireless access point. Monitors associated with this study represented the Head, Right Leg, Left Leg, Lumbar and Torso.



Figure 12: Tab Structure of Mobility Lab

The monitor labels were listed under the Setup tab and the ID numbers were inputted into the Monitor ID column as can be seen listed in Table 6. Figure 12 shows the selection of different Mobility Lab tabs: “Setup” is used to configure the monitors, “Studies” is the library of all studies, “Subjects” is the subjects in the study, “Sessions” is the type of test being performed and “Trials” is the amount of trials per session. These configurations were set up to test conditions relevant to mTBI patients and were inputted under the Setup tab.

Table 6: Monitor Labels Locations

Monitor ID	Label
163	Head
161	Left Leg
160	Lumbar
164	Right Leg
165	Trunk

Configuration of the system was done using the “un-configured” button. The system displays “not ready” in blue when there are no configurations present. Clicking this button started the configuration process. The system configured by naming the monitors with the location they are measuring and was configured once Mobility Lab prompted to undock the monitors and wait for their green light to synchronize. The status of the system changed to “configured” once all the monitors and wireless access points were in sync. All monitors blinked twice in succession every few seconds indicating that they were synchronized and transmitting. The “Ok” button was clicked to acknowledge the configuration, and the study was created. The study was called mTBI Validation.

3.5 VICON Calibration

The Vicon system was calibrated before each subject to ensure accuracy and precision. A static calibration was completed which referenced all the cameras to a calibrated L-frame (Figure 13) with reflective markers of known locations on it. A calibration wand was waved in the workspace to define and to calibrate the data collection volume. Direct linear transformations of each two –

dimensional camera view of the reflective markers were converted to real metric units in three dimensions during the dynamic calibration.

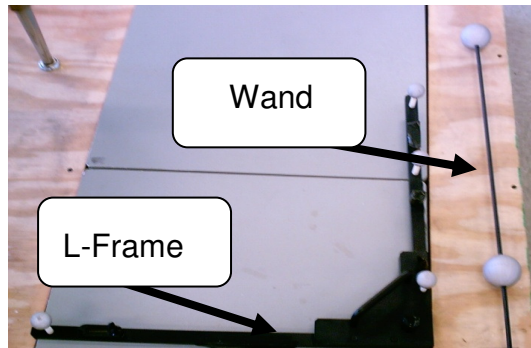


Figure 13: Calibrated Instruments

Chapter 4 - Data Analysis

4.1 APDM Data

Mobility Lab operated as a platform that ran the iTug plug-in and is the base software for recording and processing trials. The system recorded each trial based on the configuration on the iTug plug-in. The iTug operated as a modified TUG test in which the distance has been extended to seven meters instead of three due to the calculations required [5, 13, 32]. This allowed the system to calculate its parameters based on three full gait cycles. The data from the calculations are displayed in a full report generated by mobility lab.

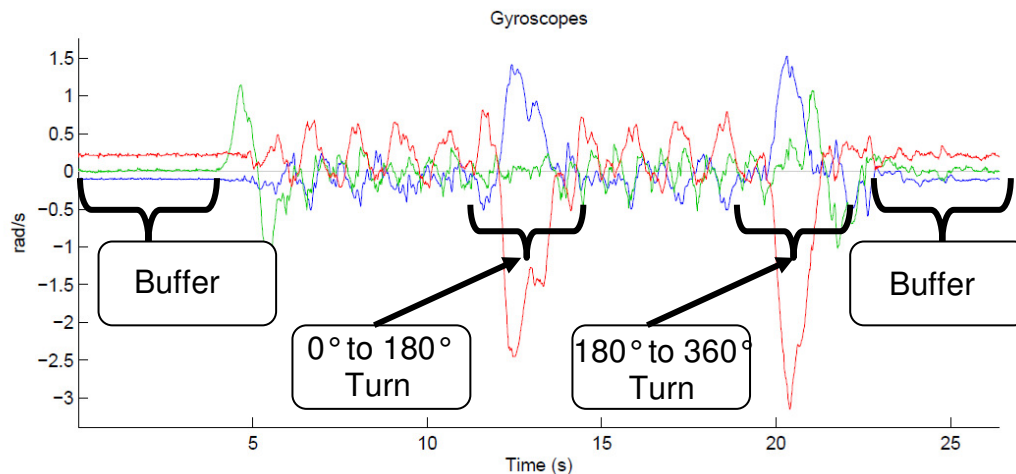


Figure 14: Trunk Gyroscope Data for Subject

The iTug plug-in started off by recording a three-second buffer time at the beginning and at the end of the trial. This required the subjects to remain still for

that duration as it recorded. These areas were known as buffer areas and were used to help eliminate the drift from the gyroscopic data during calculations. The buffer time can be seen in Figure 14 at the beginning and end of the trial. The iTug plug-in used an infinite impulse response filter to eliminate the drift associated with temperature changes and voltage fluctuations. Mobility Lab created a report based on the iTug plug-in and calculated 38 gait parameters. Mobility Lab's full report displayed all 38 gait parameters for each subject as well as the filtered data in graphical form from each monitor. Cadence, torso rate of rotation and stride length are parameters that the iTug plug-in calculated and displayed in the full report. Head rate of rotation was interpreted from graphical filtered data from a monitor mounted on the head as seen in Figure 10. The head sensor was an added feature to the iTug platform, in which it recorded the raw rate of rotation data about the Z axis.

4.1.1 Cadence

Cadence is the number of steps per minute. The iTug plug-in calculated cadence from the angular velocity of the pitch axis of the gyroscopes on the shanks. The software filtered the raw data from the shank using an infinite impulse filter that eliminates the drift, induced by changes in temperature and variations in supply voltage. The transfer function of the filter seen below has a cutoff frequency of $\alpha = 0.995$ around 0.25 hertz. The z^{-1} is the unit delay in the transfer function below.

$$H(z) = \frac{1 - z^{-1}}{1 - \alpha \times z^{-1}}$$

The signal was filtered twice, once in the forward direction and then again in the reverse direction [13, 26, 33]. The iTug algorithm gathered the data and searched it for four gait events: initial contact of the right foot, terminal contact of the left foot, initial contact of left foot and terminal contact of right foot (Figure 15). In order to locate these events, the algorithm located a positive peak point greater than 50 degrees per second. In the event that there were two peaks within 500 ms, the software chose the highest peak as the mid-swing. The next process was to search 1.5 ms before and after the mid-swing location for the initial and final contact area. The algorithm searched for the terminal and initial contact points as seen in Figure 15. The negative peak located after the mid-swing was selected as the initial contact. The initial contact happened when the heel strikes the ground. The peak points for terminal contact were small and they were filtered to smooth the signal out to locate the point. Signals were filtered using a low-pass finite impulse response filter. The frequency cutoff of this filter happened to be 30 hertz with a pass-band attenuation of less than 0.5 dB. This filter removed the erratic peak points and allowed for the selection of the terminal contact point. The local minimum prior to the mid-swing with amplitude of less than -20 degrees per second was selected [2, 5, 13, 34]. The local minimum was chosen based on previous studies, which proved that the local minimum was the initial contact of the heel [5, 31]. Figure 15 depicts the local minimum chosen. This process marked the locations of the terminal and initial contact points. The algorithm counted the number of steps in the time sequence in the trial and excluded the turns from

the data set. Exclusion criteria were based on using the sternum monitor to determine when the turns were happening.

Measuring the change in angle of the body provided the turn information. The angular velocity data from the sternum monitor about the roll axis was integrated to give the angle, then used to measure the position of the body while walking. As the subject walked forward, their angle was roughly 0 degrees. If the sternum angle changed from 0 to 180 degrees, it signified the subject performed a turn, and if the torso angle changed from 180 to 360 degrees, it signified the subject performed the second turn at the end of the trial before sitting on the chair.

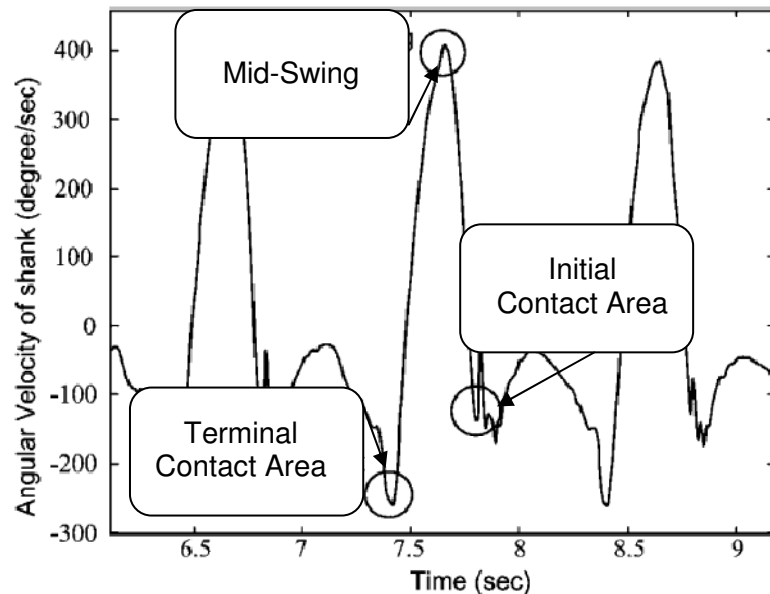


Figure 15: Sample Foot Movement [2, 5]

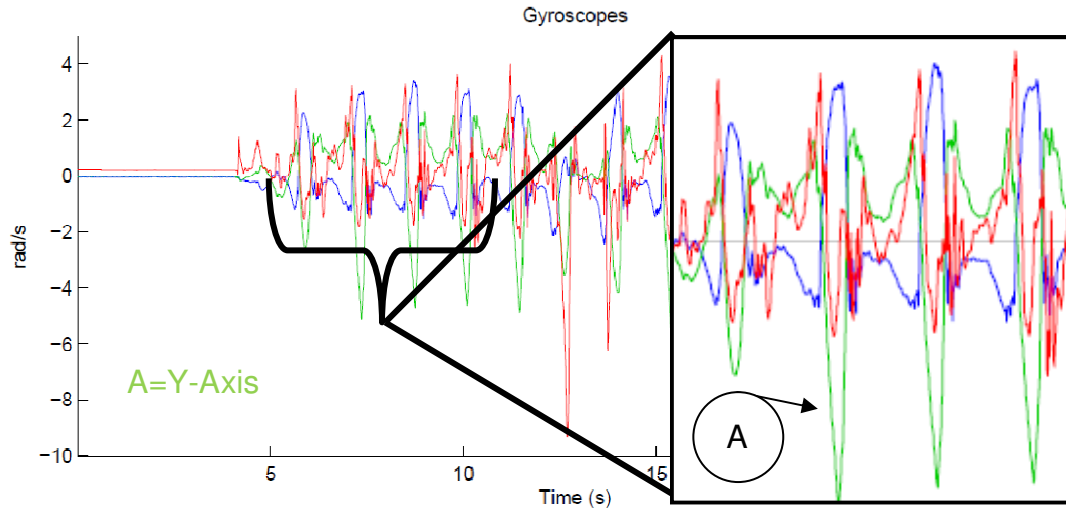


Figure 16: Zoom in on Right Leg Data of One Subject Trial

The “A” in Figure 16 represents the Y axis or pitch axis of the right shank monitor. Each heel strike was considered a step and was recorded using the iTug algorithm. The number of steps completed by the left and right shanks were added up, and divided by the time to complete those steps. The average cadence was displayed in Mobility Lab and was also plotted against the normative data provided by the company’s gait library in Figure 17.

Trials did not last more than 60 seconds and were generally less. The formula below was used to convert the amount of steps in a given time period to steps per minute.

$$\frac{\text{Steps}}{\text{Second}} * \frac{60 \text{ Seconds}}{1 \text{ Minute}} = \frac{\text{Steps}}{\text{Minute}}$$

Upon converting the data to steps per minute, the data was displayed using Mobility Lab’s full report. Cadence was displayed as a bar graph and displayed under the M row which represents the mean of cadence over the entire trial as depicted in Figure 17 [13]. The data was compared to normative data

collected by the manufacturer's gait library. This comparison was not needed for this study.

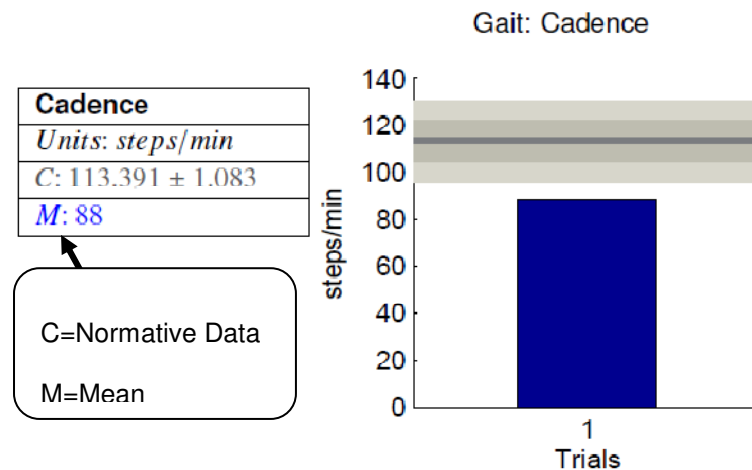


Figure 17: Cadence from Mobility Lab

4.1.2 Torso Rate of Rotation

Torso rate of rotation was a parameter that the iTug plug-in calculated and defined as peak turn velocity. This occurred when the subject walked down the seven meter walkway and turned 180 degrees to come back. As the subject walked down the seven meter walkway and approached the turn, the turn was measured by using the roll axis of the sternum monitor, seen in Figure 18. The algorithm integrated the angular velocity to calculate the angle change of the body. This angle change represented the movement of the body and detected the turn. Once the turn was detected, the algorithm measured the peak velocity. The subject's body rotation while walking from the chair was roughly 0 degrees, and as they completed the turn, the angle was 180 degrees. The angle change from 0 to 180 degrees was considered the act of the turn, and once complete, the subject had changed directions. Upon coming back to the chair, the subject

stopped and continued the rotation until they accomplished a rotation from 180 to 360 degrees before they sat down.

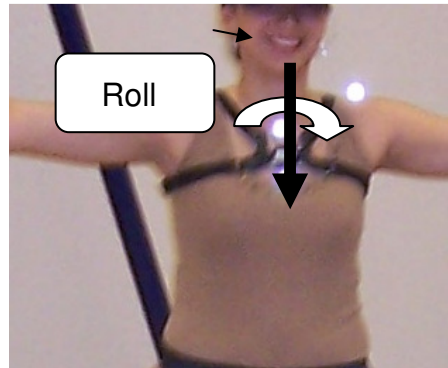


Figure 18: Yaw Representation on Sternum Monitor

Figure 14 depicts the turn event and its magnitude. Mobility Lab recorded the raw data in radians per seconds and converted it to degrees per second. The full report generated a bar graph that displayed the peak turn velocity in Figure 19. The peak turn velocities were represented as negative values, due to subjects turning in the opposite direction. As a result, the magnitude of the rate of the turn was taken and used.

The graph in Figure 19 displayed the peak turn velocity as compared to normative data, which was gathered by the manufacture library of subjects. The ranges of normative data are displayed in C, and are represented on the graph itself as the shaded regions [13]. Normative data for peak turn velocity was not used in this study.

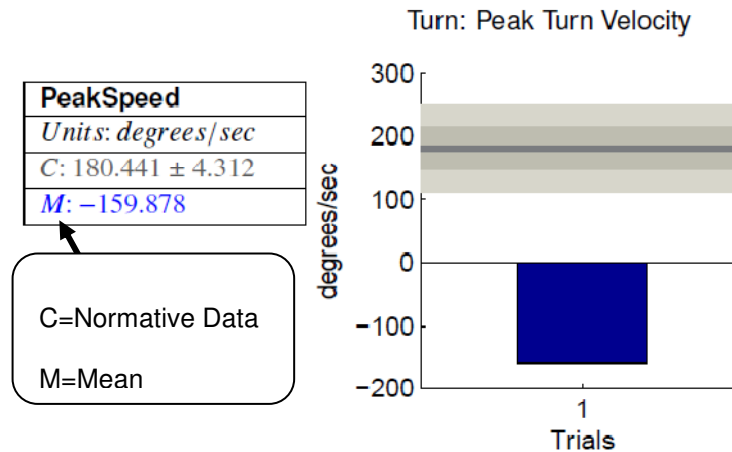


Figure 19: Peak Turn Velocity in Mobility Lab

4.1.3 Head Rate of Rotation

The head monitor was intentionally mounted on the crown of the head to provide a central axis of rotation for the system, thus eliminating the need for translation calculations between the data from Vicon and the APDM data. By keeping the axis central to each person, the rotation was always about that axis. Figure 20 depicts the axis of the model from Vicon and that of the APDM monitor are collinear. The gyroscope within the monitor produced a raw rate of rotation in radians per second, and was filtered using an infinite impulse response filter to remove the drift in the system. Keeping the monitor central to the head provided an accurate result in conjunction with the Vicon system's axis which was centrally located on the crown as well, and was the Z axis which was perpendicular to the floor.



Figure 20: Head Monitor Rotation on Subject

All of the maximum (every positive peak) and minimum (every negative peak) values on the graph were added up and averaged. The turn (0 to 180 degrees) and turn to sit (180-360 degrees) readings were excluded from the data as the head was not shifting back and forth consistently at those locations. Each subject's range of motion of the head was not controlled, but the rate at which their head was shifting from the left to right was. To help coordinate subjects' head movements during the trials, a metronome was utilized to generate a tone at specific intervals of time. Table 5 shows the speeds used to set the metronome.

Head rate of rotation was interpreted from graphical filtered data from a monitor mounted on the head as seen in Figure 21. The head sensor was an added feature to the iTug platform in which the raw rate of rotation data about the Z axis was recorded. Figure 21 demonstrates the maximums and minimums in the data and the cyclical pattern of the subjects' head. Each peak point was a representation of when the subject's head turned over to the left or the right. Positive peaks were to the left while negative peaks were when the head turned to the right.

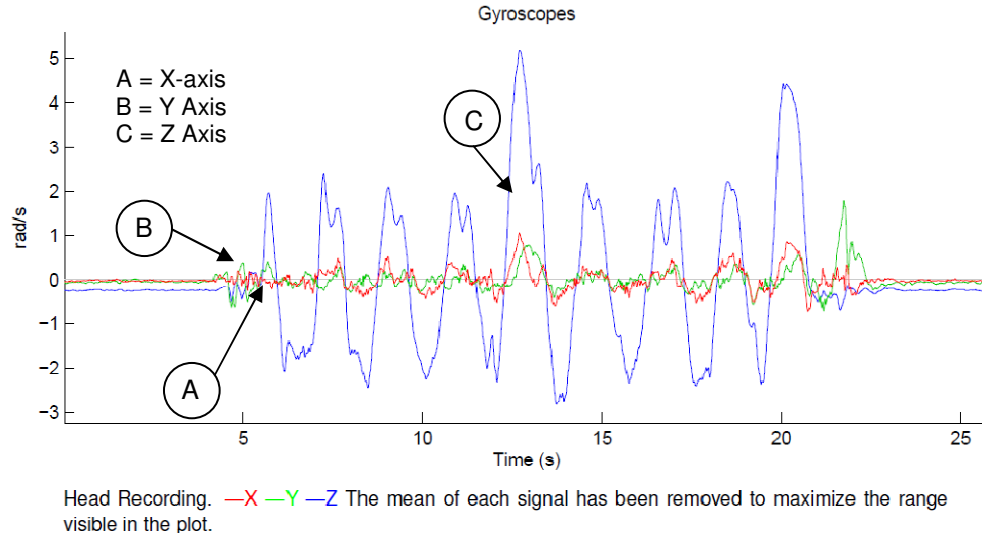


Figure 21: Filtered Gyroscope Head Data

Head rate of rotation was manually interpreted from a plot of filtered data from the head-mounted monitor. The measurements were in radians per second and gathered from Figure 21. It was then converted to degrees per second in Table 7.

$$\frac{Deg}{Sec} = \frac{Rad}{Sec} \times \left(\frac{180}{\pi} \right)$$

Table 7: Maximum and Minimum Peaks of Head

Maximum and Minimum Peaks of Head			
Rad/Sec		Deg/Sec	
Max	Min	Max	Min
2.00	2.00	114.59	114.59
2.10	2.50	120.32	143.24
2.00	2.20	114.59	126.05
2.00	3.00	114.59	171.89
2.10	2.50	120.32	143.24
2.00	2.50	114.59	143.24
2.10	2.50	120.32	143.24
Average		Average	
2.25		128.92	

4.1.4 Stride Length

Stride length is the distance between two successive placements of the same foot and is composed of a swing phase and stance phase. However, the iTug algorithm calculates stride length as a temporal parameter. The calculations were based off the time it takes to perform the stride length. The iTug plug-in calculates stride length using percent stature; which is a percentage of the subjects' body height used to describe the stride length. Stance and swing are considered components of a gait cycle, and when added together, they make up the entire gait cycle. The definition of stance is the phase of a gait cycle that begins with the strike of a heel and ends with the lift of the toe of the same leg. Swing phase was defined as the foot off the ground and started after the stance phase.

Stride length was calculated using the gyroscope data from the shank monitors of both legs. The system used the angular velocity about the pitch (Y) axis from both of the gyroscopes on the shank. iTug filtered the data from the shank initially using a high pass infinite impulse response filter to eliminate the drift from the gyroscopes. The procedure listed in section 4.1.1 (cadence) was replicated to detect the initial contact of the heel and the final contact of the toe. The formulas below used the initial contact of the right foot ($IC_R(k)$) and terminal contact of the right foot ($TC_R(k)$) which is shown in Figure 15. The process of acquiring and processing the shank data was the same for stride length as was with cadence, and the same calculations for both the left and right sides of the body were done.

A double pendulum model was used to calculate the stride length as a function of percent stature as seen in Figure 22, and to represent human motion. The model for swing was a pendulum, while stance was an inverted pendulum. The inverted pendulum states the model was rotated 180 degrees. Each model required the position angles of the legs, which was derived from integrating the angular rate of rotation with respect to time.

This program operated with the assumption that the left and right steps were of equal lengths, therefore, suggesting that the rotations during the left stance phase were equal to the rotations during the right stance phase.

The process below of calculating stride length had been tested and validated [31]. The temporal parameter of d_3 is the distance the body moved between the start of the stance and the end of the stance. The distance in the swing before the stance is d_1 and the distance after the stance is d_2 . The darker lines of the pendulum model show the movement of the right foot, while the thin line represents the left foot [2, 5, 13, 34]. As subjects start the gait cycle, the right heel strikes the ground while the left heel was ready for toe off. In the next step, the left heel moved into swing, while the right transferred into stance. The left foot then contacted the ground for a heel strike as the right went into swing. The gait cycle is over once the left heel contacted the ground and the right heel went into swing.

$$\text{Gait Cycle Time} = GCT(k) = IC_R(k + 1) - IC_R(k)$$

The double pendulum model was a simplified version of human gait and did not factor in double support because the model represented the shank and

the thigh, and the heel was not modeled. In order to calculate gait cycle time, the difference between the initial contact and the initial contact of the next gait cycle was calculated for the same foot.

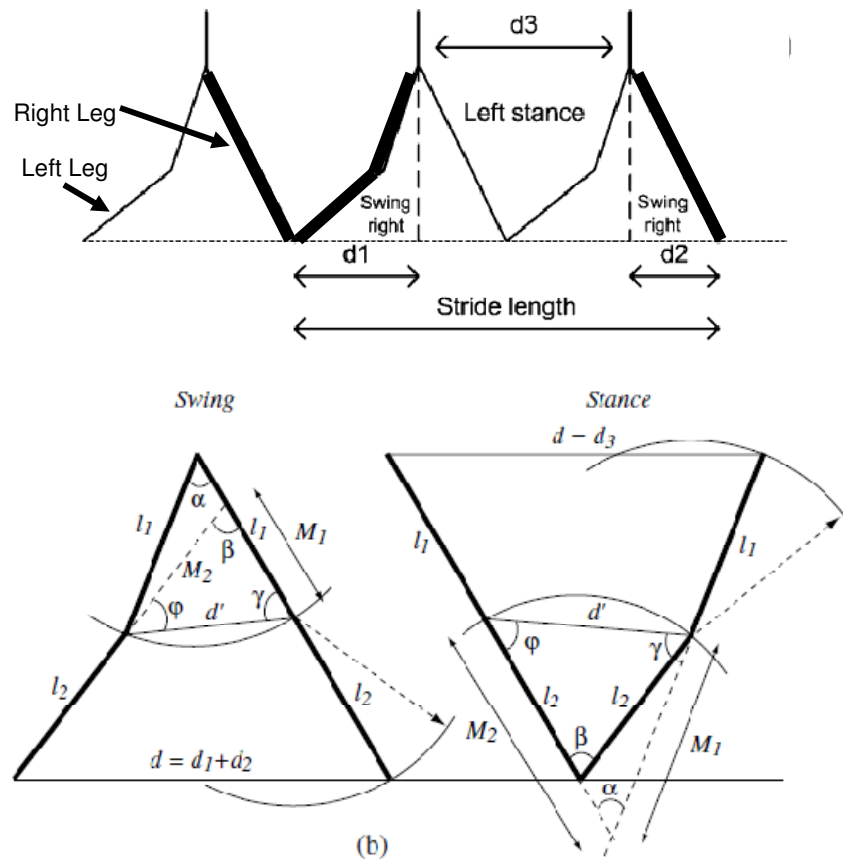


Figure 22: Pendulum Model of Stride Length [13, 26]

The formulas used to describe this are listed below for one side of the body [5, 13]. This algorithm was applied to the stride lengths on both legs. This algorithm used estimations of the thigh angular rotations, as well as the leg lengths, which were based on an average of leg lengths taken by the manufacturers gait libraries of human subjects. The equations below were used to compute swing distance [5, 34].

$$\text{Stance (\%)} = d_3$$

$$\text{Swing (\%)} = d_1 + d_2$$

$$\text{Stride Length (\% Stature)} = d_1 + d_2 + d_3$$

$$M_1 = \frac{\sin \varphi(k)}{\sin \beta(k)} d'(k)$$

$$M_2 = \frac{\sin \gamma(k)}{\sin \beta(k)} d'(k)$$

In the equations above, M_1 is the radius of the thigh swing, while M_2 is the radius of the shank swing. The angular velocity recorded from the shank monitor was integrated to compute $\beta(k)$. The angle $\alpha(k)$ is the angular rotation of the thigh and was interpreted from the shank monitor. The angular rotation of the thigh was based on the relationship between the shank monitor and normative data collected by the manufacturer [13, 31]. In the equations below, the angles of $\varphi(k)$ and $\gamma(k)$ were computed from the angles of $\alpha(k)$ and $\beta(k)$. The formulas below show the relationship between the integrated angles and the angles needed for the inverse pendulum model. Figure 22 shows the pendulum models used in the calculations of $\gamma(k)$, $\varphi(k)$, M_1 and M_2 and all these formulas require $d'(k)$ which was based on the leg length l_1 [5, 34].

$$\gamma(k) = \frac{\pi - \alpha(k)}{2} d'(k)$$

$$\varphi(k) = \frac{\pi - 2\beta(k) + \alpha(k)}{2} d'(k)$$

$$d'(k) = l_1 \sqrt{2(1 - \cos \alpha(k))}$$

Once all the angles were computed, the swing phase was calculated based on the angular rotation of the shank known as $\beta(k)$ [5, 34]. Percent

stature in swing was calculated using the law of cosines which encompasses the components of leg lengths and their respective angles to find the distance as a temporal parameter as seen in the equation below. It is dependent on the time of the gait cycle of that event.

$$d_{1+2}(k) = d_1(k) + d_2(k)$$

$$d_{1+2}(k) = \sqrt{(l_2 + M_1(k))^2 + (l_2 + M_2(k))^2 - (l_2 + M_1(k))(l_2 + M_2(k)) \cos \beta(k)}$$

Stance is the remainder of the gait cycle and is the bulk of the stride length. The model for stance is an inverse pendulum model that uses a different leg length (l_2) to compute the angles of rotation in the legs during the phase as seen in Figure 22. In the equations below, the angles of $\varphi(k)$ and $\gamma(k)$ were computed from the angles of $\alpha(k)$ and $\beta(k)$, which are dependent on l_2 and $\beta(k)$ in the equation $d'(k)$. Distances for the thigh and shank were still represented as M_1 and M_2 , but $d'(k)$ is dependent on l_2 . The same process for computing the swing phase was applied to the stance phase. The process starts off with recording the angular velocity from the shank monitor and then was integrated to compute $\beta(k)$. Angle $\beta(k)$ was calculated based on the angular rotation of the shank monitor and $\alpha(k)$ was used from the swing phase [13, 31]. The formula for the angles and the components it depends on are given below [5, 34].

$$\gamma(k) = \frac{\pi - \beta(k)}{2} d'(k)$$

$$\varphi(k) = \frac{\pi - 2\alpha(k) + \beta(k)}{2}d'(k)$$

$$d'(k) = l_2(k)\sqrt{2(1 - \cos \beta(k))}$$

Once all the angles have been calculated, the stance equation was used to provide the final component to stride length. Stance was calculated using the law of cosines formula that relates the angles to the lengths of the sides of legs. Stance distance was calculated as a temporal parameter, and was dependent on the time of the gait cycle of that event. The equation used to calculate stance is listed below [5, 34].

$$d_3(k) = \sqrt{(l_1 + M_2(k))^2 + (l_1 + M_1(k))^2 - (l_1 + M_2(k))(l_1 + M_1(k)) \cos \alpha(k)}$$

Once both swing and stance have been calculated using the law of cosines, they both are added together to provide the stride length in percent stature [2, 5, 13, 34].

$$\text{Stride Length (\% Stature)} = d_1 + d_2 + d_3$$

Mobility Lab displayed this metric in percent stature in the full report as seen in Figure 23. In order to record the stride length as an actual value in meters, the percent stature was converted using the formula below in Excel. The height of the subject was multiplied by the percent stature to compute the stride length in meters as shown in following equation:

$$\text{Stride Length (meters)} = (\text{Percent Stature (\%)}) \times (\text{Subject Height(meters)})$$

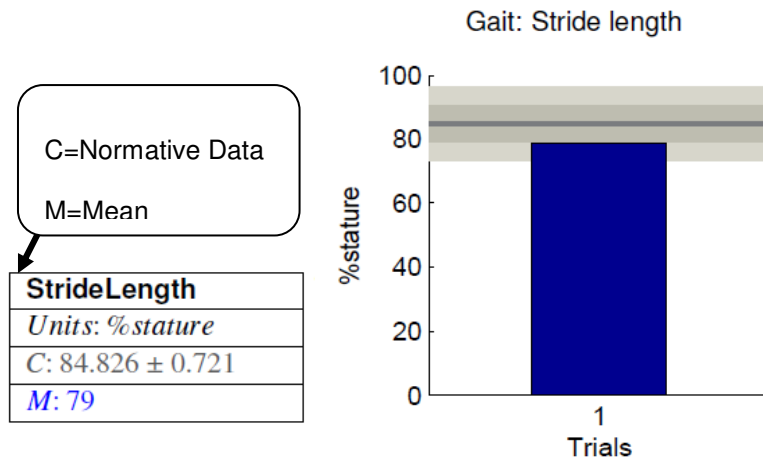


Figure 23: Stride Length from Mobility Lab

4.2 VICON Data

Data collected from the Vicon System were calculated using Visual 3D. Visual 3D by C-Motion processed all the data at once using a custom algorithm developed for this study, known as a pipeline. Visual 3D took the raw data from the Vicon Workstation and applied the pipeline to it. The algorithm (Appendix A) utilized the labels provided in Table 4 to base its calculations off of. Each trial was brought into Visual 3D and grouped based on the trial and session. The set of algorithms in the pipeline mimicked what the iTug plug-in computed. In the event that the algorithm (Appendix A) did not compute the parameters correctly, plots were used to manually calculate the desired parameters. Plots were created for each case when the algorithm did not work, and the points of interest on the plots were recorded in Excel and processed. The plots in each section from Visual 3D had event markers in them that represented heel strikes and toe offs.

4.2.1 Cadence

Cadence was calculated in Visual 3D using the pipeline. Cadence was calculated by measuring the number of heel strikes (steps) that happened in a given time frame. Both the left and the right foot had to be accounted for in cadence. The algorithm (Appendix A) located the path of the heel marker with respect to the pelvis and marked the heel strike as an “event maximum” as well as the toe off as an “event minimum”. Once the path was determined and the event markers located, the algorithm computed the time along the x axis that it took to complete one stride. The algorithm then counted all the strides and excluded the turns. One stride was calculated as: heel strike of right heel marker, toe off of left toe marker and heel strike of right heel marker. This metric was in steps per seconds for one leg. These numbers were taken into Excel and were converted to steps per minute. This represented the cadence of one leg, and to get the overall cadence, both left and right cadence values are added together. The pipeline replicated the same algorithm for each subject.

In order to check the functionality of the process above, and to compute the desired parameter in the event of an error, a manual method was used. The Z component was used to measure the gait cycle of the heel marker. The assumption of symmetry was valid for healthy subjects, but in this study, an average of both sides was taken into account to eliminate the assumption of symmetry. The algorithm plotted the graph of a heel marker in the z axis against time. Counting the number of gait cycles in a time frame excluding the turns gave the total number of steps. This provided the amount of steps in a time frame

which had to be converted to steps per minute. Figure 24 shows the right heel marker taken by Vicon. Both the left and the right heel markers are being displayed in Figure 25..

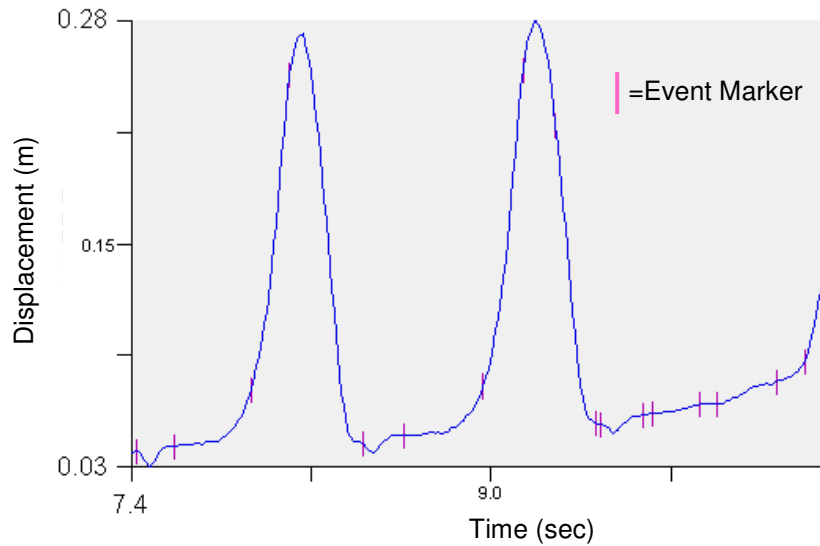


Figure 24: Right Heel Marker on Vicon

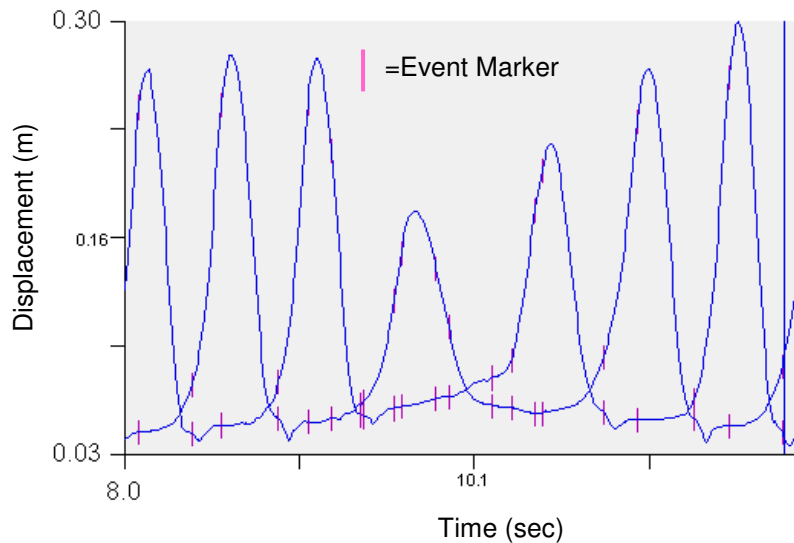


Figure 25: Left and Right Heel Marker on Vicon Joined

Turns were visualized using the playback function of Visual 3D to confirm the exclusion criteria, and to replicate the exclusion criteria that the iTug plug-in

performed. A sample calculation below was used to demonstrate this principle. Figure 25 shows that the first heel strike happened at 8.1 seconds and ended at 12 seconds and the turn started at 9.4 seconds and ended at 10.8 seconds. The number of steps within that time frame is 6 steps

$$\frac{6 \text{ Steps}}{((13 - 8.0) - (11 - 9.0)) \text{ Seconds}} = \frac{6 \text{ Steps}}{3 \text{ Seconds}} = \frac{2 \text{ Steps}}{1 \text{ Second}}$$

$$\frac{2 \text{ Steps}}{1 \text{ Second}} \times \frac{60 \text{ Seconds}}{1 \text{ Minute}} = 120 \frac{\text{Steps}}{\text{Minute}}$$

This number was simplified and then multiplied against the conversion factor.

4.2.2 Torso Rate of Rotation

Torso rate of rotation is the rate of rotation about the pelvis relative to the floor. The pelvis was used in this study because it drove the torso rotation at the end of the walkway. The torso rotated with the pelvis at this point. The pelvis plane was found using the markers on the pelvis (posterior superior iliac spine and anterior superior iliac spine of the left and right); this was used to create a plane and to find the central axis rate of rotation. The pelvis plane was parallel to the calibrated lab floor, and the axis of rotation (yaw axis) in question was perpendicular to the floor. The peak turn velocity of the pelvis was determined by measuring the maximum turn velocity at the first turn in the algorithm (Appendix A); this was when the subject turned 180 degrees at the end of the walkway. The algorithm searched for the joint velocity at the turn and filtered the data using a Butterworth filter to smooth out the data. The rate of rotation throughout the trial

was not desired and therefore was excluded during the gait phase between the turns.

In the event the algorithm did not compute the peak turn velocity, a manual method using the angular velocity plot of the pelvis was utilized. A plot of the pelvis axis was created and analyzed for the highest rate of rotation about the turn as seen in Figure 26. For example the highest point was approximately 171.9 degrees per second. This measurement unit matched that of APDM and was recorded in Excel

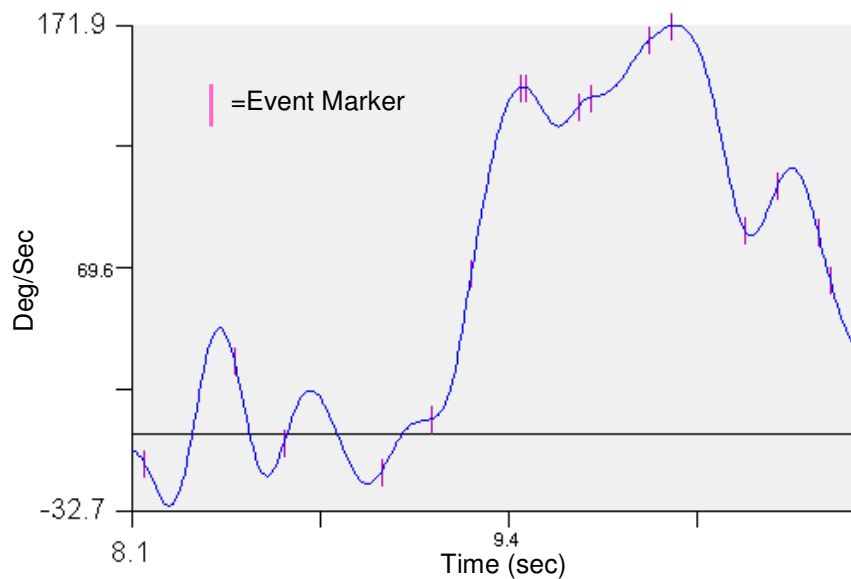


Figure 26: Rate of Rotation of the Torso

4.2.3 Head Rate of Rotation

The head rate of rotation was constantly being monitored throughout each subject's trial and only the data from the turns were excluded from the calculations. To calculate the head rate of rotation, a plane was created using the

head markers. The markers created a plane whose central axis was collinear with that of the APDM Opal Monitor as seen in Figure 27. As the subject performed the trials, the plane rotated about the central axis. Figure 28 shows the maximum (all the positives) and minimum (all the negatives) peaks throughout a segment of time in the trial. The algorithm (Appendix A) searched for these peaks and recorded them. The marker sets used were the two markers on the front and the two on the back of the head. The algorithm calculated the joint velocity about the central axis (Z axis) and this axis was perpendicular to the global coordinate frame which was the floor.

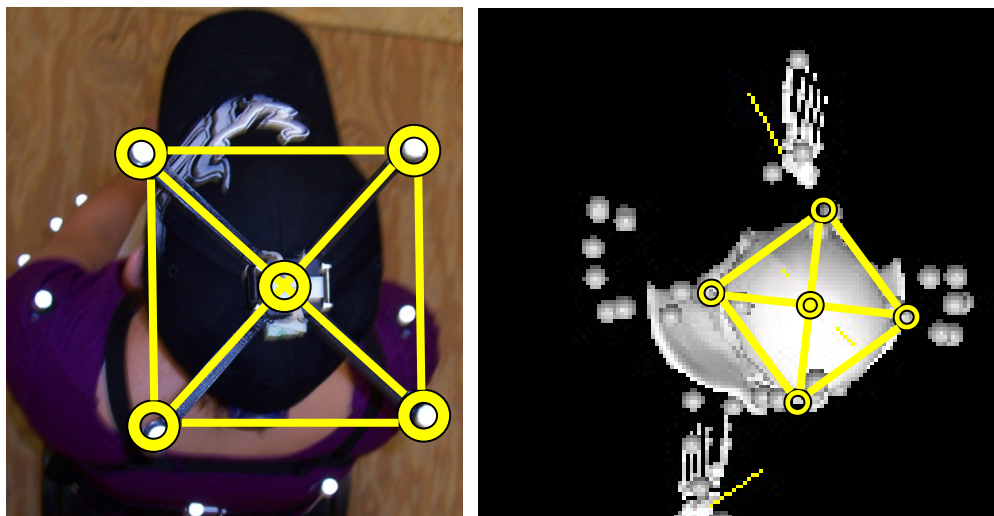


Figure 27: Plane of Markers on Subject's Head

The data were then taken into Excel and processed for irregularities such as outliers. Medians of the data were used to eliminate the irregularities gathered. An example of an outlier can be seen in Figure 28 where there are two peak points within the same amplitude.

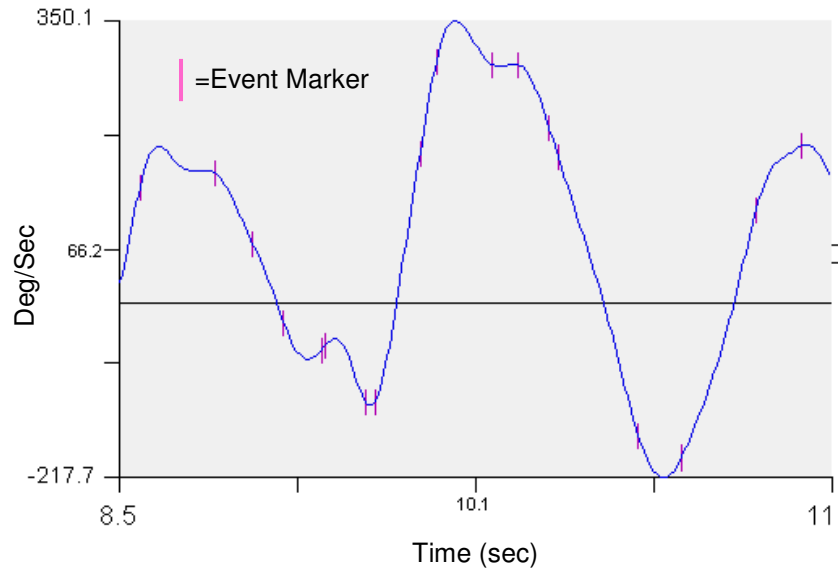


Figure 28: Vicon Head Rotation about Central Axis

By using the median, the dual peaks were eliminated. Examples of the calculations used to eliminate the outliers are in Table 8.

Table 8: Head Rate of Rotation Data

Head Rate of Rotation					
Trial	Deg/Sec	Median	Trial	Deg/Sec	Median
Slow walk 1	133.79	128.84	Fast walk 1	239.19	245.46
	123.89			251.74	
	142.89		Fast walk 2	190.85	190.85
	123.57		Fast walk 3	147.50	147.50
Slow walk 2	118.40	118.40			
Slow walk 3	121.98	121.98			
	156.00				
	105.87				

4.2.4 Stride Length

The distance between two successive heel strikes of the same foot is a stride length. The model of the right side was used to explain the algorithm

(Appendix A). The sequence of marker events that were used to measure the distance and calculate the stride length along the x axis were the right heel strike, right toe off, and the next right heel strike. The algorithm measured the distance between those three event markers and calculated the stride for that gait cycle. Once again, the turns were excluded from the calculations to resemble the APDM output. The data was then exported to Excel for further processing and to eliminate the outlier data by using the medians. The process was replicated for the left side as well. The average of the two stride lengths gave the average stride length for the subject.

In the event that Visual 3D didn't compute the needed parameters, a manual method was used by interpreting the displacement plot (Figure 29). The two heel strikes were marked on the graph for each gait cycle, Once they were marked, the displacement between the initial heel contact and the second same-heel contact points were measured as the stride length. The differences between the plateaus where the heel strikes occur are the actual stride length of the gait cycle. An example of how this was calculated manually is seen below.

$$\text{Stride Length(meters)} = |2\text{nd Initial Contact} - \text{Initial Contact}|$$

$$\text{Stride Length (meters)} = |1.1 \text{ meters} - (-0.1) \text{ meters}| = 1.2 \text{ meters}$$

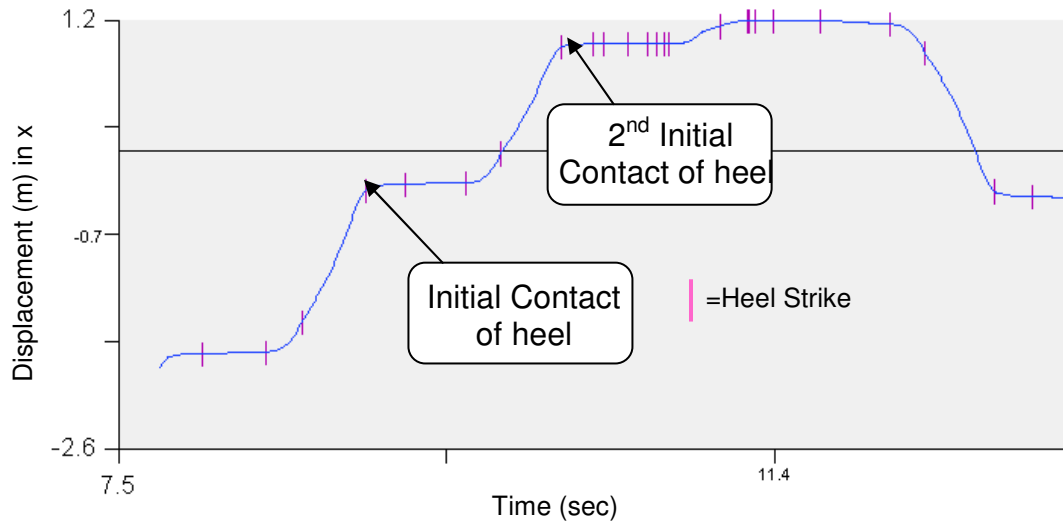


Figure 29: Stride Length of Right Foot

4.3 Correlation

Correlating the two systems against one another will validate the APDM system to some degree, which was the goal of this project. The strength of the correlation was determined using the Pearson's R correlation [35].

Table 9: Correlation Values for Pearson's R Correlation

Correlation Value	
0-0.2	Low Correlation
0.2-0.5	Slight Correlation
0.5-0.7	Moderate Correlation
0.7-1	High Correlation

The desired correlation value for a perfectly correlated system is 1 and an absolute no correlation value is 0. If the correlation value is positive, both sets of data increase together, and if a negative correlation occurs, one data set increases while the other decreases. The breakdown of the correlation values

are given in Table 9. The formula used to compute the Pearson's R correlation is as follows:

$$R = \frac{N \sum xy - (\sum x)(\sum y)}{\sqrt{[N \sum x^2 - (\sum x)^2][N \sum y^2 - (\sum y)^2]}}$$

The x terms refer to one system such as the APDM system and the y terms refer to the other system such as the Vicon system. Within each system there are four parameters that were compared. Where N represents the number of pairs of scores from the data, $\sum xy$ represents the sum of the products of paired scores, $\sum x$ represents the sum of the x scores, $\sum y$ represents the sum of the y scores, $\sum x^2$ represents the sum of squared x scores from the data, and $\sum y^2$ represents the sum of squared y scores from the data. In order to plot the results of the correlation values the R the scales of both systems would be required. The R value is multiplied by this difference in scale to attain the true slope. Since the scales of both systems are the same for each parameter, the R value determined would be the slope of the best fit line. There was no standardization which meant that there was no technical standard given. An example of standardized data would be comparing a new product using the same components such as USB's and Ethernet ports.

Data gathered from each system was utilized uniquely within each software platform. The data from APDM was processed using Mobility Lab, while with the Vicon system, Visual 3D was used to process the raw data into the four parameters desired for this study.

Chapter 5 - Results

This study aimed at validating the APDM system against the Vicon system using the Pearson's R correlation. The study correlated cadence, torso rate of rotation, head rate of rotation and stride length. Correlation values, R, are given as follows:

$$R = \frac{N \sum xy - (\sum x)(\sum y)}{\sqrt{[N \sum x^2 - (\sum x)^2][N \sum y^2 - (\sum y)^2]}}$$

Subjects performed three trials of each session and each set was averaged to minimize the effect of poor trials. This average was used to represent the subject's gait parameters selected for this study. Correlation values were computed in SPSS and plotted accordingly. The Pearson's R correlation was used to test the strength of each gait parameter in respect to each system. Plots were created for all correlation values for each session as well as the overall value. Both data sets were brought into Excel (Microsoft Office) and SPSS (IBM) and compared to one another.

5.1 Cadence Correlation

Cadence data from the Vicon system were converted to match that of the APDM system. Data was taken from the reports of both the Mobility Lab and the Visual 3D programs and inputted into Table 10. This table represents all the trial

averages from each subject and subject's standard deviations. The correlation was calculated for each session followed by an overall correlation value of the entire parameter.

Table 10: Average Trials for Cadence

		Normal Avg Steps/Min	Std dev	Fast Avg Steps/Min	Std dev	Slow Avg Steps/Min	Std dev
H1	APDM	100	1.00	113	1.73	85	2.52
	Vicon	100	1.66	112	0.46	86	2.41
H2	APDM	101	2.89	107	1.73	87	3.21
	Vicon	97	2.37	106	4.70	89	4.45
H3	APDM	105	0.00	108	3.21	82	1.53
	Vicon	103	1.18	103	2.04	86	6.15
H4	APDM	107	2.65	113	4.16	84	3.79
	Vicon	103	2.32	116	5.54	88	4.38
H5	APDM	102	1.53	112	0.58	83	0.58
	Vicon	101	2.35	114	4.44	85	0.90
H6	APDM	102	2.00	111	1.53	86	3.06
	Vicon	98	2.96	110	2.37	86	5.26
H7	APDM	108	1.00	120	1.15	90	2.52
	Vicon	107	3.48	118	2.50	100	7.55
H8	APDM	106	4.16	116	1.15	98	2.08
	Vicon	106	2.69	113	4.27	98	4.60
H9	APDM	117	2.65	127	4.58	112	1.53
	Vicon	112	1.97	123	4.66	116	5.25
H10	APDM	108	0.00	112	1.53	86	2.08
	Vicon	105	1.61	111	1.38	86	3.17

Table 11: Cadence Correlation Values

Cadence Correlation	
Session	R
Normal	0.935
Fast	0.918
Slow	0.895
Overall	0.967

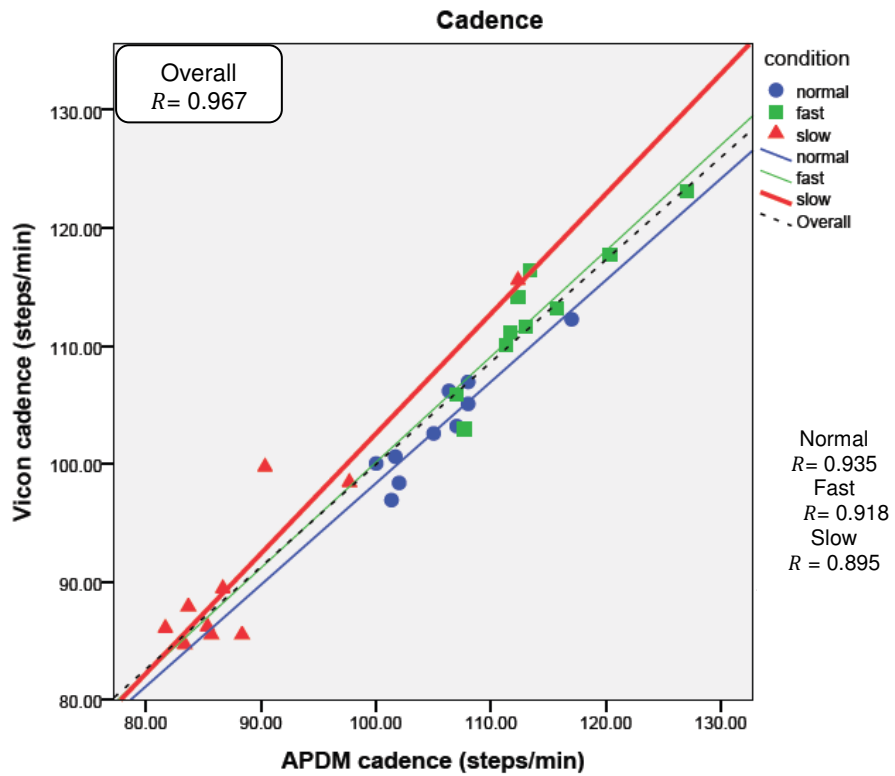


Figure 30: Correlation Graph of Cadence

The correlation values are given in Table 11 for each session as well as the overall correlation value of the parameter. All three sessions were plotted in Figure 30 and the overall correlation value was plotted as well. The R value was the measure of linear dependence between two variables and was represented

dotted line in Figure 30. The overall correlation value was $R = 0.967$. The cadence was highly correlated between the two systems.

5.1.1 Torso Rate of Rotation Correlation

Torso rate of rotation was recorded in fast and slow sessions. The data was taken from Mobility Lab and the Visual 3D program and inputted into Excel and SPSS. The rates of rotation are displayed in Table 12 as well as the standard deviation for each average.

Table 12: Average Rate of Rotation for the Torso

		Normal Avg	Std dev	Fast Avg	Std dev	Slow Avg	Std dev
H1	APDM	201.75	3.65	268.73	18.41	164.81	10.73
	Vicon	188.87	11.88	281.42	22.30	157.46	23.72
H2	APDM	202.52	20.40	202.52	20.40	233.55	14.08
	Vicon	190.87	7.43	230.50	17.54	225.63	17.04
H3	APDM	176.08	22.23	197.71	9.29	168.08	11.45
	Vicon	204.74	12.60	239.65	26.45	157.08	9.10
H4	APDM	204.17	5.08	219.68	28.15	220.79	13.55
	Vicon	219.50	13.03	249.01	53.80	244.47	22.88
H5	APDM	182.64	24.07	240.94	21.67	179.03	7.56
	Vicon	194.28	21.93	251.69	17.72	206.90	12.27
H6	APDM	141.11	10.70	208.97	30.26	144.87	37.13
	Vicon	148.70	12.93	237.61	12.62	136.20	20.63
H7	APDM	181.85	4.94	148.94	2.53	146.04	12.99
	Vicon	186.51	6.76	169.47	3.26	152.94	14.80
H8	APDM	295.74	21.56	249.07	44.91	206.40	8.56
	Vicon	311.80	16.44	231.01	24.78	208.59	14.82
H9	APDM	218.71	19.94	241.36	37.90	223.14	22.07
	Vicon	205.44	14.01	249.19	58.17	236.01	33.49
H10	APDM	178.36	9.33	209.84	13.37	176.23	31.68
	Vicon	181.64	13.65	249.09	27.27	182.61	35.06

Table 13: Torso Rate of Rotation Correlation Values

Torso Rate of Rotation Correlation	
Session	R
Normal	0.955
Fast	0.851
Slow	0.940
Overall	0.907

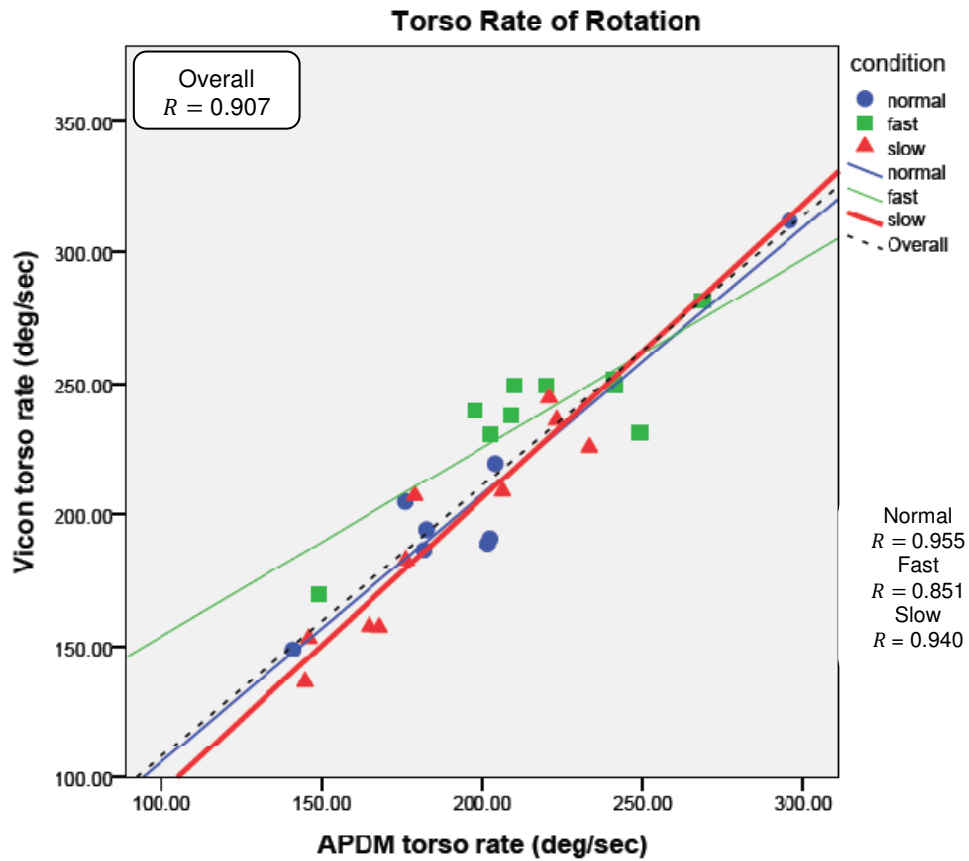


Figure 31: Correlation for Rate of Rotation for Torso

The correlation values are given in Table 13 for each session as well as the overall correlation value of the parameter. All sessions were plotted in Figure 31 and the overall correlation value was plotted as well. The R value was the

measure of linear dependence between two variables and was represented dotted line in Figure 31. The overall correlation value was $R = 0.907$. The torso rate of rotation for was highly correlated between the two systems.

5.1.2 Head Rate of Rotation Correlation

The head rate of rotation data were taken from Visual 3D and converted from the charts in Mobility Lab. Tables of the average head rate of rotation per trial were created in Excel. Data was then brought into SPSS for processing and calculating the Pearson's R correlation. The averages are in tabular form as seen in Table 14. Standard deviations are displayed in conjunction with averages.

Table 14: Average Rate of Rotation for Head

		Fast Avg Deg/Sec	Std dev	Slow Avg Deg/Sec	Std dev
H1	APDM	205.25	13.55	136.92	7.13
	Vicon	188.19	28.29	127.75	5.31
H2	APDM	233.55	14.08	219.39	30.87
	Vicon	255.69	43.17	161.86	30.60
H3	APDM	148.47	12.04	126.53	9.27
	Vicon	158.94	55.51	131.44	24.31
H4	APDM	198.70	44.95	100.97	2.27
	Vicon	229.50	23.02	109.68	9.34
H5	APDM	310.22	57.61	199.54	13.25
	Vicon	322.79	13.70	193.36	52.22
H6	APDM	270.44	4.77	176.39	4.13
	Vicon	230.59	15.57	184.63	16.70
H7	APDM	240.85	23.33	215.22	10.12
	Vicon	236.87	32.27	183.87	67.98
H8	APDM	171.30	10.47	148.61	12.32
	Vicon	158.75	0.15	142.04	24.26
H9	APDM	283.31	21.63	225.08	2.12
	Vicon	275.66	44.29	202.36	28.97
H10	APDM	333.23	19.16	194.23	24.46
	Vicon	338.44	22.01	197.05	27.28

Table 15: Head Rate of Rotation Correlation Values

Head Rate of Rotation Correlation	
Session	R
Fast	0.942
Slow	0.884
Overall	0.942

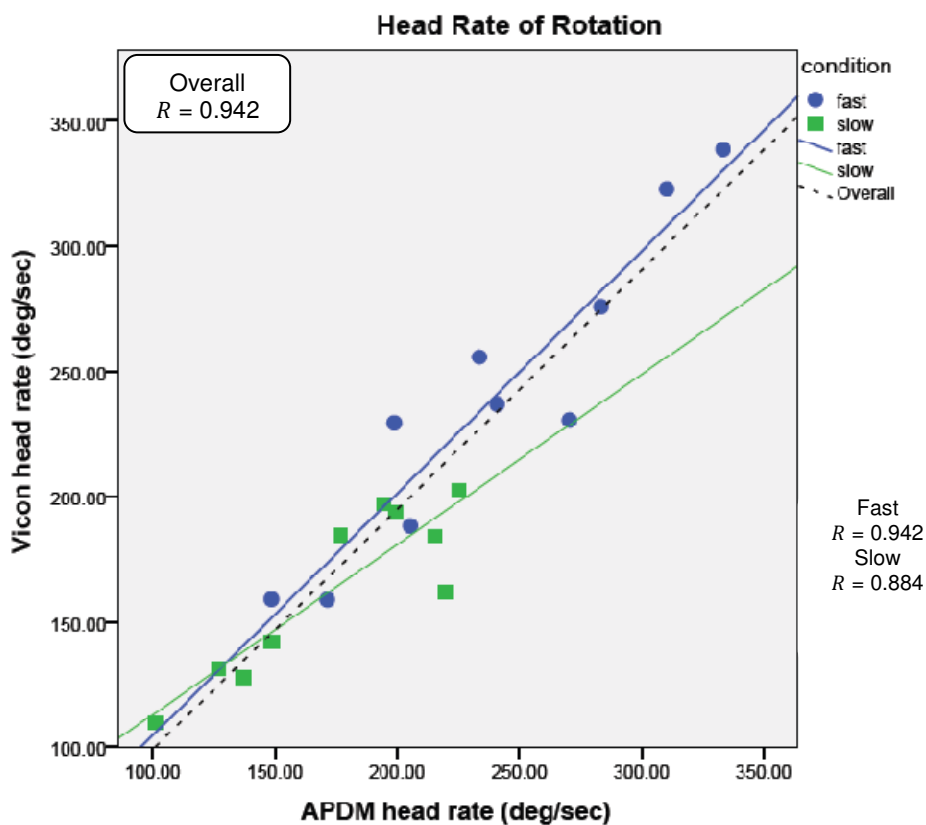


Figure 32: Correlation for Rate of Rotation of the Head

The correlation values are given in Table 15 for each session as well as the overall correlation value of the parameter. Both sessions were plotted in Figure 32 and the overall correlation value was plotted as well. The R value was the measure of linear dependence between two variables and was represented

dotted line in Figure 32. The overall correlation value was $R=0.942$, indicating high correlation between both systems for head rate of rotation.

5.1.3 Stride Length Correlation

Stride length was calculated in Excel from the reports of APDM and Visual 3D. Data was put into tabular form for processing and calculation in SPSS. The averages of all the trials were taken as well as the standard deviations displayed in Table 16.

Table 16: Average Stride Length

		Normal Avg	Std Dev	Fast Avg	Std Dev	Slow Avg	Std Dev
H1	APDM	1.59	0.05	1.66	0.02	1.41	0.02
	Vicon	1.50	0.04	1.84	0.04	1.28	0.02
H2	APDM	1.48	0.06	1.51	0.04	1.42	0.03
	Vicon	1.41	0.03	1.59	0.04	1.28	0.01
H3	APDM	1.41	0.02	1.44	0.02	1.35	0.06
	Vicon	1.31	0.02	1.46	0.02	1.21	0.10
H4	APDM	1.54	0.03	1.63	0.02	1.44	0.02
	Vicon	1.46	0.05	1.49	0.07	1.29	0.01
H5	APDM	1.41	0.04	1.45	0.03	1.28	0.03
	Vicon	1.28	0.03	1.28	0.03	1.09	0.04
H6	APDM	1.59	0.02	1.58	0.02	1.38	0.03
	Vicon	1.35	0.01	1.46	0.04	1.08	0.05
H7	APDM	1.42	0.01	1.42	0.04	1.36	0.01
	Vicon	1.16	0.05	1.25	0.05	1.03	0.02
H8	APDM	1.48	0.02	1.46	0.00	1.39	0.02
	Vicon	1.32	0.01	1.29	0.02	1.11	0.02
H9	APDM	1.34	0.00	1.31	0.05	1.17	0.04
	Vicon	1.27	0.07	1.22	0.12	0.94	0.04
H10	APDM	1.35	0.01	1.48	0.02	1.24	0.02
	Vicon	1.20	0.01	1.32	0.02	1.00	0.06

Table 17: Stride Length Correlation Values

Stride Length Correlation	
Session	R
Normal	0.776
Fast	0.8
Slow	0.817
Overall	0.861

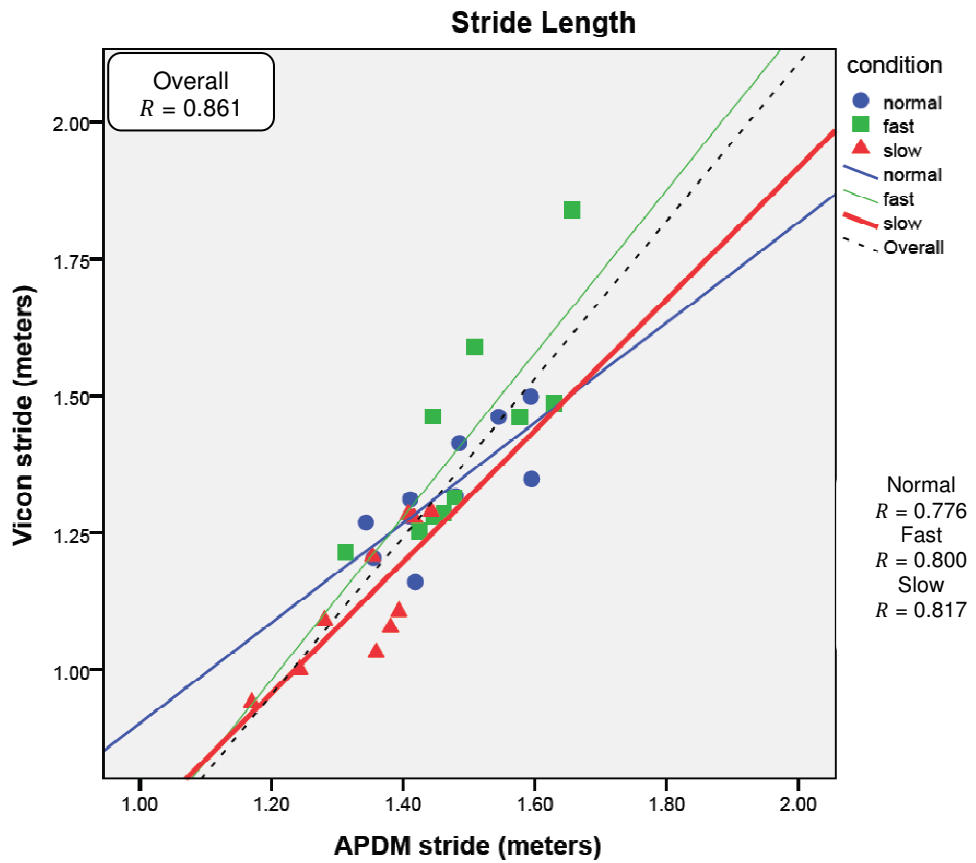


Figure 33: Correlation for Stride Length

The correlation values are given in Table 17 for each session as well as the overall correlation value of the parameter. Both sessions were plotted in

Figure 33 as well as the overall correlation value. The R value was the measure of linear dependence between two variables and was represented dotted line in Figure 33. The overall Pearson's R correlation value was $R=0.861$ and highly correlated between both systems. Normal and fast sessions were moderately correlated, while the slow session had the highest correlation value.

Chapter 6 - Discussion and Limitations

6.1 Discussion

The results of this study demonstrated the correlation between the Vicon and APDM systems in terms of the following parameters: cadence, torso rate of rotation, head rate of rotation and stride length; all of which are highly correlated as seen in Table 18. The values calculated from the iTug algorithm were accurate representations of subject's selected gait parameters as compared to the Vicon system. The correlation values for each session were computed to show the difference within each session as compared to the overall correlation value. By computing the overall correlation values for a parameter, a more accurate representation of the parameter was computed.

Table 18: Pearson's R Correlation Values

Cadence			Torso Rate of Rotation		
Normal	Fast	Slow	Normal	Fast	Slow
0.935	0.918	0.895	0.955	0.851	0.94
Overall		0.967	Overall		0.907
Stride Length			Head Rate of Rotation		
Normal	Fast	Slow		Fast	Slow
0.776	0.8	0.817		0.942	0.884
Overall		0.861	Overall		0.942

Adding more data points to a calculation gives a better representation of what the data is doing. The APDM system was very accurate in collecting and calculating the gait parameters for this study, but the correlation values could have been slightly higher if some of the ways that the iTug algorithm computed the data were different.

Controlling the subjects' speed could have led to a greater correlation values. What may have caused the lower correlations was the fact that the speeds were self selected, and each individual changed speed differently; some individuals increased their cadence while some increased their stride length. Different combinations of this caused different outcomes on how gait speed was controlled. A solution to this may include controlling the speed on a treadmill, this would have allowed for consistency throughout the subjects' testing sessions.

One of the lowest correlation values was from the stride length parameter. Gathering stride length from a gyroscope can be tricky and generally ends up introducing more errors into the calculation due to drift. Using the shank to represent the heel can be inaccurate in this model due to the fact that movements of the shank and the heel are not the same between individuals. Mounting the APDM monitor on the actual heel could have led to a better representation of the subjects' leg.

APDM's iTug may have introduced a slight error into the system with the use of gyroscopes. The exact locations of the gyroscopes on the body play an important role in measuring a segment properly, and could lead to errors if not placed properly. These errors could result in wrong angles calculated or wrong

stride lengths calculated. The process of computing the stride length (percent stature) from the shank monitors was not direct. The algorithm utilized average leg lengths and average thigh movements in conjunction with the actual subject shank data to calculate stride length. The algorithm used these estimated lengths to calculate critical angles in the double pendulum model. This method was not completely accurate because of subjects' differing body segment lengths and movements. As a result, stride length required the most computation in order to reach the desired value in APDM's iTug plug-in. This gave the calculations a higher chance at picking up an error and transferring it through to the result. A solution that could have increased the accuracy of this algorithm would be to measure the actual leg length of the subject and to include it in the calculations instead of the average data. By increasing the accuracy of the results, the correlation values could have slightly increased. This modification would only result in a slight increase due to thigh movements being estimated.

Another potential solution to the low correlation value of stride length would be to calibrate the APDM monitors prior to each subject's trial. The calibration process would utilize the same two shank monitors and have the subjects' walk down a pathway of a known distance. The physical stride length would be calibrated with that of the APDM system's stride length and would add a calibration factor that would be applied to all the subject's trials.

The final possible method for increasing the stride length correlation would be to use four monitors instead of two and to use the actual leg lengths from the subject. This would increase precision and accuracy in the pendulum model's

stance phase and swing phase. Monitors would be placed on both sides of the shanks and thighs; and by placing the monitors on the thigh, a better representation of what the thigh motion is can be measured. This method is more direct than the iTug's version and would be significantly more accurate.

However the stride length parameter can still be considered to be accurate and highly correlated against the Vicon system. Another parameter that can have better correlation values is the head rate of rotation. Calculating the rate of rotation of the head was not an automated process, which also added human error into the calculations. Manually calculating the peaks was not efficient and not clinically appropriate. Automating this process would decrease the human error and improve accuracy. Placing the devices on the central axis of the head removed the need for axis transformation for this calculation. In the event the monitor was mounted on the forehead or the back of the head, transformation formulas would have to be used to relate the position of the monitor to the central location.

Overall, this study suggested that the parameters of cadence, torso rate of rotation, head rate or rotation and stride length are valid parameters that could be used to monitor gait parameters associated with mild traumatic brain injury.

6.2 Limitations

This study included few limitations in the APDM system as well as in the Vicon system:

1. A small sample size was chosen, and a bigger sample size would have smoothed out the data.
2. Healthy subjects were used and not subjects with an mTBI.
3. Data from the angular velocity of the gyroscope still had to be mathematically integrated, adding slight errors to the calculations.
4. Determination of stride length required calibration.
5. When subjects walked too fast or ran, their data would not be calculated due to noise in the monitors.
6. APDM's iTug did not compute average head rate of rotation because it was not a parameter common to Parkinson's disease. Manual calculation of the head rate of rotation was necessary, which introduced some human error.
7. Mobility Lab reports are long and report far more parameters than are needed for this application. Separating the needed parameters was time consuming.
8. Vicon system requires an extensive setup and a controlled laboratory.
9. Vicon was not portable and it requires additional hardware.
10. Vicon requires a controlled lighting environment and must be calibrated after every subject trial session.

Chapter 7 - Conclusion and Future Work

7.1 Conclusion

This study aimed to validate commercially available wearable sensor system to monitor selected gait parameters against a gold standard system. The APDM system was chosen for its low cost, portability and its ability to be used in outdoor environments [2]. Validation of the APDM system against the Vicon system was performed using four parameters relevant to mild traumatic brain injury: cadence, torso rate of rotation, head rate of rotation and stride length [1, 7]. Ten healthy subjects between 20 -27 years of age completed this study by performing three different gait sessions. Correlations between the systems were done using these parameters and the Pearson's R correlation formula.

The correlation values for cadence, head rate of rotation and torso rate of rotation were found to be high between both systems. Out of all the correlation values, stride length was the lowest but was still highly correlated, and was potentially low because stride length was not calibrated specifically for each individual subject; the information for performing this calibration was not available at the time of this study. A later study could show the potential increase in correlation with this enhanced calibration. Overall, the APDM Movement Monitor system was found to be valid against the gold standard of the Vicon system for

the selected parameters, and would be a great addition for clinician to use on subjects in or out of the laboratory.

7.2 Future Work

Future work on this topic would include the validation of the APDM system by testing it with actual mTBI subjects. This study validated four common parameters relevant to mTBI. Testing subjects with an mTBI using the same study parameters and comparing the data against the normal population would provide insight on how well the system works for subjects exhibiting abnormalities.

Generating an mTBI plug-in for APDM's Mobility Lab software would also be necessary for the task of testing mTBI subjects. The plug-in would incorporate a head sensor that would be applied to the algorithm and generate a smaller report with the desired parameters, which would increase its clinical utility.

By using the accelerometers in conjunction with the gyroscopes, the gait events could be located more accurately. The system can be used to view the different periods of a subject's gait cycle. Measuring the accelerations of certain body segments can provide an accurate location of an event, and be used to view different periods of a subject's gait cycle, including but not limited to mid-swing, terminal contacts, initial contacts, swing, pre-swing and loading response.

References

- [1] Williams, G., Morris, M. E., Schache, A., 2009, "Incidence of Gait Abnormalities After Traumatic Brain Injury," *Archives of Physical Medicine and Rehabilitation*, 90(4) pp. 587-593.
- [2] Aminian, K., and Najafi, B., 2004, "Capturing Human Motion using Body-Fixed Sensors: Outdoor Measurement and Clinical Applications," *Computer Animation and Virtual Worlds*, 15(2) pp. 79-94.
- [3] Yang, C., and Hsu, Y., 2010, "A Review of Accelerometry-Based Wearable Motion Detectors for Physical Activity Monitoring," *Sensors*, 10(8) pp. 7772-7788.
- [4] Sosnoff, J., Broglio, S., and Ferrara, M., 2008, "Cognitive and Motor Function are Associated Following Mild Traumatic Brain Injury," *Experimental Brain Research*, 187(4) pp. 563-571.
- [5] Salarian, A., Russmann, H., Vingerhoets, F. J. G., 2004, "Gait Assessment in Parkinson's Disease: Toward an Ambulatory System for Long-Term Monitoring," *Biomedical Engineering, IEEE Transactions on*, 51(8) pp. 1434-1443.
- [6] Bhimji, S., 2000, "Static and Dynamic Accuracy of the VICON 370 3-D Kinematic System," *Gait Posture*, 11(2) pp. 130.
- [7] Williams, G., Galna, B., Morris, M. E., 2010, "Spatiotemporal Deficits and Kinematic Classification of Gait Following a Traumatic Brain Injury: A Systematic Review," *The Journal of Head Trauma Rehabilitation*, 25(5) pp. 366-374 10.1097/HTR.0b013e3181cd3600.
- [8] Aggarwal, J. K., and Cai, Q., 1997, "Human motion analysis: a review," *Nonrigid and Articulated Motion Workshop, 1997. Proceedings.*, IEEE, Anonymous pp. 90-102.
- [9] Pontifex, M. B., O'Connor, P. M., Broglio, S. P., 2009, "The Association between Mild Traumatic Brain Injury History and Cognitive Control," *Neuropsychologia*, 47(14) pp. 3210-3216.

- [10] R., B., CHOU Li-Shan, R., K., 2003, "An Assessment of Gait and Balance Deficits After Traumatic Brain Injury," 84(1) pp. 7.
- [11] Medley, A., Thompson, M., and French, J., 2006, "Predicting the Probability of Falls in Community Dwelling Persons with Brain Injury: A Pilot Study," Brain Inj, 20(13-14) pp. 1403-1408.
- [12] Podsiadlo, D., and Richardson, S., 1991, "The Timed "Up and Go"; A Test of Basic Functional Mobility for Frail Elderly Persons," J Am Geriatr Soc, 39pp. 142-188.
- [13] Salarian, A., Horak, F. B., Zampieri, C., 2010, "ITUG, a Sensitive and Reliable Measure of Mobility," Neural Systems and Rehabilitation Engineering, IEEE Transactions on, 18(3) pp. 303-310.
- [14] Vasterling, J. J., Verfaellie, M., and Sullivan, K. D., 2009, "Mild Traumatic Brain Injury and Posttraumatic Stress Disorder in Returning Veterans: Perspectives from Cognitive Neuroscience," Clinical Psychology Review, 29(8) pp. 674-684.
- [15] Chou, L., Kaufman, K. R., Walker-Rabatin, A. E., 2004, "Dynamic Instability during Obstacle Crossing Following Traumatic Brain Injury," Gait & Posture, 20(3) pp. 245-254.
- [16] Kaufman, K. R., Brey, R. H., Chou, L., 2006, "Comparison of Subjective and Objective Measurements of Balance Disorders Following Traumatic Brain Injury," Medical Engineering & Physics, 28(3) pp. 234-239.
- [17] Kunju, N., Kumar, N., Pankaj, D., 2009, "Algorithm for Kinematic Measurements using Active Markers," Advance Computing Conference, 2009. IACC 2009. IEEE International, Anonymous pp. 387-391.
- [18] Karen, K., 2011, Consultant at Veterans Affairs Hospital, U.S.A., private communication.
- [19] Privateer, P. M., 1999, "Academic Technology and the Future of Higher Education: Strategic Paths Taken and Not Taken," The Journal of Higher Education, 70(1) pp. pp. 60-79.
- [20] Wilson, J., 2009, "A Practical Approach to Vibration Detection and Measurement," 2011(2/15) .
- [21] Takeda, R., Tadano, S., Todoh, M., 2009, "Gait Analysis using Gravitational Acceleration Measured by Wearable Sensors," Journal of Biomechanics, 42(3) pp. 223-233.

- [22] Narayanan, M. R., Redmond, S. J., Scalzi, M. E., 2010, "Longitudinal Falls-Risk Estimation using Triaxial Accelerometry," Biomedical Engineering, IEEE Transactions on, 57(3) pp. 534-541.
- [23] David, A., and Michael, H., 2007, "Introduction to Mechatronics and Measurement Systems," McGraw-Hill Companies, .
- [24] Alvarez, D., Gonzalez, R. C., Lopez, A., 2006, "Comparison of Step Length Estimators from Wearable Accelerometer Devices," Engineering in Medicine and Biology Society, 2006. EMBS '06. 28th Annual International Conference of the IEEE, Anonymous pp. 5964-5967.
- [25] Yeoh, W., Pek, I., Yong, Y., 2008, "Ambulatory monitoring of human posture and walking speed using wearable accelerometer sensors," Engineering in Medicine and Biology Society, 2008. EMBS 2008. 30th Annual International Conference of the IEEE, Anonymous pp. 5184-5187.
- [26] Miyazaki, S., 1997, "Long-Term Unrestrained Measurement of Stride Length and Walking Velocity Utilizing a Piezoelectric Gyroscope," Biomedical Engineering, IEEE Transactions on, 44(8) pp. 753-759.
- [27] Tong, K., and Granat, M. H., 1999, "A Practical Gait Analysis System using Gyroscopes," Medical Engineering & Physics, 21(2) pp. 87-94.
- [28] Baroni, G., Ferrigno, G., and Pedotti, A., 1998, "Implementation and Application of Real-Time Motion Analysis Based on Passive Markers," Medical and Biological Engineering and Computing, 36(6) pp. 693-703.
- [29] Sementille, A. C., Louren\cco, L. E., Brega, J. R. F., 2004, "A motion capture system using passive markers," Proceedings of the 2004 ACM SIGGRAPH international conference on Virtual Reality continuum and its applications in industry, Anonymous ACM, New York, NY, USA, pp. 440-447.
- [30] Webster, K. E., Wittwer, J. E., and Feller, J. A., 2005, "Validity of the GAITRite® Walkway System for the Measurement of Averaged and Individual Step Parameters of Gait," Gait & Posture, 22(4) pp. 317-321.
- [31] Barker, S., Craik, R., Freedman, W., 2006, "Accuracy, Reliability, and Validity of a Spatiotemporal Gait Analysis System," Medical Engineering & Physics, 28(5) pp. 460-467.
- [32] Salarian, A., Russmann, H., Vingerhoets, F. J. G., 2007, "Ambulatory Monitoring of Physical Activities in Patients with Parkinson's Disease," Biomedical Engineering, IEEE Transactions on, 54(12) pp. 2296-2299.

- [33] Lavry, D., 1997, "Understanding IIR (Infinite Impulse Response) Filters - an Intuitive Approach," 2011(06/10) pp. 5.
- [34] Aminian, K., Najafi, B., Büla, C., 2002, "Spatio-Temporal Parameters of Gait Measured by an Ambulatory System using Miniature Gyroscopes," Journal of Biomechanics, 35(5) pp. 689-699.
- [35] Montgomery, D., and Runger, G., 2010, "Applied Statistics and Probability for Engineers," Wiley, John & Sons, Incorporated, .

Appendices

Appendix A - Pipeline

Start of Pipeline

```
/EVENT_NAME=BoT  
/FRAME=1  
!/TIME=  
;
```

```
Event_Explicit  
/EVENT_NAME=EoT  
/FRAME=EOF -50  
!/TIME=  
;
```

Computes the head joint velocity using the head plane which consists of the two front and two back head markers

```
Compute_Model_Based_Data  
/RESULT_NAME=HeadRotRate  
/FUNCTION=JOINT_VELOCITY  
/SEGMENT=RHE  
!/REFERENCE_SEGMENT=LAB  
/RESOLUTION_COORDINATE_SYSTEM=  
!/USE_CARDAN_SEQUENCE=FALSE  
!/NORMALIZATION=FALSE  
!/NORMALIZATION_METHOD=  
!/NORMALIZATION_METRIC=  
!/NEGAITEX=FALSE  
!/NEGAITEY=FALSE  
!/NEGAITEZ=FALSE  
!/AXIS1=X  
!/AXIS2=Y  
!/AXIS3=Z  
;
```

Converts the head rate of rotation to degrees per second from radians per second

```
Multiply_Signals_By_Constant  
/SIGNAL_TYPES=LINK_MODEL_BASED  
/SIGNAL_NAMES=HeadRotRate  
!/SIGNAL_FOLDER=ORIGINAL  
/RESULT_NAMES=HeadRateRad  
/RESULT_TYPES=LINK_MODEL_BASED  
!/RESULT_FOLDER=PROCESSED  
!/RESULT_SUFFIX=  
!/SIGNAL_COMPONENTS=  
/CONSTANT=pi()/180
```


Appendix A (Continued)

Computes the pelvis rate of rotation using the two Asis and 2 Psis markers as a plane. The joint velocity of this plane is calculated. The pelvis drives the rotation of the torso on the turn.

```
Compute_Model_Based_Data
/RESULT_NAME=LumbarRateRot
/FUNCTION=JOINT_VELOCITY
/SEGMENT=RPV
!/REFERENCE_SEGMENT=LAB
/RESOLUTION_COORDINATE_SYSTEM=
!/USE_CARDAN_SEQUENCE=FALSE
!/NORMALIZATION=FALSE
!/NORMALIZATION_METHOD=
!/NORMALIZATION_METRIC=
!/NEGAITEX=FALSE
!/NEGAITEY=FALSE
!/NEGAITEZ=FALSE
!/AXIS1=X
!/AXIS2=Y
!/AXIS3=Z
;
```

Applies a low pass filter to smooth out the data for the rotation of the pelvis

```
Lowpass_Filter
/SIGNAL_TYPES=LINK_MODEL_BASED
/SIGNAL_NAMES=LumbarRateRot
!/SIGNAL_FOLDER=ORIGINAL
!/RESULT_SUFFIX=
!/RESULT_FOLDER=PROCESSED
!/FILTER_CLASS=BUTTERWORTH
/FREQUENCY_CUTOFF=3
!/NUM_REFLECTED=6
!/TOTAL_BUFFER_SIZE=6
!/NUM_BIDIRECTIONAL_PASSES=1
;
```

Converts the pelvis rate of rotation to degrees per second from radians per second

```
Multiply_Signals_By_Constant
/SIGNAL_TYPES=LINK_MODEL_BASED
/SIGNAL_NAMES=LumbarRateRot
!/SIGNAL_FOLDER=ORIGINAL
/RESULT_NAMES=LumbarRateRotRad
/RESULT_TYPES=LINK_MODEL_BASED
!/RESULT_FOLDER=PROCESSED
!/RESULT_SUFFIX=
!/SIGNAL_COMPONENTS=
/CONSTANT=pi()/180
;
```

Appendix A (Continued)

Applies a low pass filter to smooth out the data for the lumbar rate of rotation

```
Lowpass_Filter
/SIGNAL_TYPES=LINK_MODEL_BASED
/SIGNAL_NAMES=LumbarRateRotRad
/SIGNAL_FOLDER=PROCESSED
!/RESULT_SUFFIX=
!/RESULT_FOLDER=PROCESSED
!/FILTER_CLASS=BUTTERWORTH
/FREQUENCY_CUTOFF=3
!/NUM_REFLECTED=6
!/TOTAL_BUFFER_SIZE=6
!/NUM_BIDIRECTIONAL_PASSES=1
;
```

Applies a low pass filter to smooth out the data for the head rate of rotation

```
Lowpass_Filter
/SIGNAL_TYPES=LINK_MODEL_BASED
/SIGNAL_NAMES=HeadRotRate
/SIGNAL_FOLDER=ORIGINAL
!/RESULT_SUFFIX=
!/RESULT_FOLDER=PROCESSED
!/FILTER_CLASS=BUTTERWORTH
/FREQUENCY_CUTOFF=3
!/NUM_REFLECTED=6
!/TOTAL_BUFFER_SIZE=6
!/NUM_BIDIRECTIONAL_PASSES=1
;
```

Computes the target path of the left toe marker in respect to the Pelvis plane

```
Compute_Model_Based_Data
/RESULT_NAME=LTOE_WRT_PELVIS
/FUNCTION=TARGET_PATH
/SEGMENT=LTOE
/REFERENCE_SEGMENT=RPV
/RESOLUTION_COORDINATE_SYSTEM=RPV
!/USE_CARDAN_SEQUENCE=FALSE
!/NORMALIZATION=FALSE
!/NORMALIZATION_METHOD=
!/NORMALIZATION_METRIC=
!/NEGAITEX=FALSE
!/NEGAITEY=FALSE
!/NEGAITEZ=FALSE
!/AXIS1=X
!/AXIS2=Y
!/AXIS3=Z
;
```

Appendix A (Continued)

Computes the target path of the left heel marker in respect to the Pelvis plane

```
Compute_Model_Based_Data
/RESULT_NAME=LHEE_WRT_PELVIS
/FUNCTION=TARGET_PATH
/SEGMENT=LHEE
/REFERENCE_SEGMENT=RPV
/RESOLUTION_COORDINATE_SYSTEM=RPV
!/USE_CARDAN_SEQUENCE=FALSE
!/NORMALIZATION=FALSE
!/NORMALIZATION_METHOD=
!/NORMALIZATION_METRIC=
!/NEGAITEX=FALSE
!/NEGAITEY=FALSE
!/NEGAITEZ=FALSE
!/AXIS1=X
!/AXIS2=Y
!/AXIS3=Z
;
```

Computes the target path of the right toe marker in respect to the Pelvis plane

```
Compute_Model_Based_Data
/RESULT_NAME=RTOE_WRT_PELVIS
/FUNCTION=TARGET_PATH
/SEGMENT=RTOE
/REFERENCE_SEGMENT=RPV
/RESOLUTION_COORDINATE_SYSTEM=RPV
!/USE_CARDAN_SEQUENCE=FALSE
!/NORMALIZATION=FALSE
!/NORMALIZATION_METHOD=
!/NORMALIZATION_METRIC=
!/NEGAITEX=FALSE
!/NEGAITEY=FALSE
!/NEGAITEZ=FALSE
!/AXIS1=X
!/AXIS2=Y
!/AXIS3=Z
;
```

Appendix A (Continued)

Computes the target path of the right heel marker in respect to the pelvis plane

```
Compute_Model_Based_Data
/RESULT_NAME=RHEE_WRT_PELVIS
/FUNCTION=TARGET_PATH
/SEGMENT=RHEE
/REFERENCE_SEGMENT=RPV
/RESOLUTION_COORDINATE_SYSTEM=RPV
!/USE_CARDAN_SEQUENCE=FALSE
!/NORMALIZATION=FALSE
!/NORMALIZATION_METHOD=
!/NORMALIZATION_METRIC=
!/NEGAITEX=FALSE
!/NEGAITEY=FALSE
!/NEGAITEZ=FALSE
!/AXIS1=X
!/AXIS2=Y
!/AXIS3=Z
;
```

Locates the maximum event markers of the left heel marker with respect to the pelvis plane

```
Event_Maximum
/SIGNAL_TYPES=LINK_MODEL_BASED
/SIGNAL_NAMES=LHEE_WRT_PELVIS
!/SIGNAL_FOLDER=ORIGINAL
/EVENT_NAME=LHS
/SELECT_X=TRUE
!/SELECT_Y=FALSE
!/SELECT_Z=FALSE
/FRAME_WINDOW=20
!/START_AT_EVENT=
!/END_AT_EVENT=
/EVENT_INSTANCE=0
;
```

Locates the high event markers of the right heel marker with respect to the pelvis plane

```
Event_Maximum
/SIGNAL_TYPES=LINK_MODEL_BASED
/SIGNAL_NAMES=RHEE_WRT_PELVIS
!/SIGNAL_FOLDER=ORIGINAL
/EVENT_NAME=RHS
/SELECT_X=TRUE
!/SELECT_Y=FALSE
!/SELECT_Z=FALSE
/FRAME_WINDOW=20
!/START_AT_EVENT=
!/END_AT_EVENT=
/EVENT_INSTANCE=0
;
```

Appendix A (Continued)

Locates the low event markers of the left toe marker with respect to the pelvis plane

```
Event_Minimum
/SIGNAL_TYPES=LINK_MODEL_BASED
/SIGNAL_NAMES=LTOE_WRT_PELVIS
!/SIGNAL_FOLDER=ORIGINAL
/EVENT_NAME=LTO
/SELECT_X=TRUE
!/SELECT_Y=FALSE
!/SELECT_Z=FALSE
/FRAME_WINDOW=20
!/START_AT_EVENT=
!/END_AT_EVENT=
/EVENT_INSTANCE=0
```

Locates the low event markers of the right toe with respect to the pelvis

```
Event_Minimum
/SIGNAL_TYPES=LINK_MODEL_BASED
/SIGNAL_NAMES=RTOE_WRT_PELVIS
!/SIGNAL_FOLDER=ORIGINAL
/EVENT_NAME=RTO
/SELECT_X=TRUE
!/SELECT_Y=FALSE
!/SELECT_Z=FALSE
/FRAME_WINDOW=20
!/START_AT_EVENT=
!/END_AT_EVENT=
/EVENT_INSTANCE=0
```

Using the Z component of the Lumbar rate or rotation an event marker is placed after 65 degrees per second for the lumbar rate of rotation. Determining if the signal doesn't passes through the threshold. Meaning the turn exclusion

```
Event_Threshold
/SIGNAL_TYPES=LINK_MODEL_BASED
/SIGNAL_NAMES=LumbarRateRot
/SIGNAL_FOLDER=PROCESSED
/EVENT_NAME=Thld1
!/SELECT_X=FALSE
!/SELECT_Y=FALSE
/SELECT_Z=TRUE
!/SELECT_RESIDUAL=FALSE
/THRESHOLD=65
!/FRAME_WINDOW=8
!/FRAME_OFFSET=0
/ASCENDING=TRUE
!/DESCENDING=FALSE
/ENSURE_RANGE_FRAMES_BEFORE_THRESHOLD_CROSSING=TRUE
!/ENSURE_RANGE_FRAMES_AFTER_THRESHOLD_CROSSING=FALSE
/START_AT_EVENT=BOT
/END_AT_EVENT=EOT
```

Appendix A (Continued)

```
/EVENT_INSTANCE=1
```

Using the Z component of the Lumbar rate or rotation an event marker is placed after 65 degrees per second for the lumbar rate of rotation. Determining if the signal will pass through the threshold. Meaning the turn exclusion

```
Event_Threshold  
/SIGNAL_TYPES=LINK_MODEL_BASED  
/SIGNAL_NAMES=LumbarRateRot  
/SIGNAL_FOLDER=PROCESSED  
/EVENT_NAME=Thld2  
!/SELECT_X=FALSE  
!/SELECT_Y=FALSE  
/SELECT_Z=TRUE  
!/SELECT_RESIDUAL=FALSE  
/THRESHOLD=65  
!/FRAME_WINDOW=8  
!/FRAME_OFFSET=0  
!/ASCENDING=FALSE  
/DESCENDING=TRUE  
!/ENSURE_RANGE_FRAMES_BEFORE_THRESHOLD_CROSSING=FALSE  
/ENSURE_RANGE_FRAMES_AFTER_THRESHOLD_CROSSING=TRUE  
/START_AT_EVENT=BOT  
/END_AT_EVENT=EOT  
/EVENT_INSTANCE=1  
;
```

Computes the maximum value of the head rate of rotation using the head plane and stores the value as a metric

```
Metric_Maximum  
/RESULT_METRIC_NAME=MaxHeadRot  
!/APPLY_AS_SUFFIX_TO_SIGNAL_NAME=FALSE  
!/RESULT_METRIC_FOLDER=PROCESSED  
/SIGNAL_TYPES=LINK_MODEL_BASED  
/SIGNAL_NAMES=HeadRotRate  
!/SIGNAL_FOLDER=PROCESSED  
/SIGNAL_COMPONENTS=Z  
/EVENT_SEQUENCE=LHS+LTO+LHS  
/EXCLUDE_EVENTS=Thld1+Thld2  
/GENERATE_MEAN_AND_STDDEV=FALSE  
!/APPEND_TO_EXISTING_VALUES=FALSE  
!/CREATE_GLOBAL_MAXIMUM=FALSE  
;
```

Appendix A (Continued)

Computes the maximum value of the pelvis plane rotation and store the values as a metric

```
Metric_Maximum
/RESULT_METRIC_NAME=MaxTorsoRot
!/APPLY_AS_SUFFIX_TO_SIGNAL_NAME=FALSE
!/RESULT_METRIC_FOLDER=PROCESSED
/SIGNAL_TYPES=LINK_MODEL_BASED
/SIGNAL_NAMES=LumbarRateRot
/SIGNAL_FOLDER=PROCESSED
/SIGNAL_COMPONENTS=Z
/EVENT_SEQUENCE=Thld1+Thld2
/EXCLUDE_EVENTS=
/GENERATE_MEAN_AND_STDDEV=FALSE
!/APPEND_TO_EXISTING_VALUES=FALSE
!/CREATE_GLOBAL_MAXIMUM=FALSE
;
```

Displays the maximum torso rate of rotation from the turn in graphical form

```
Event_Maximum
/SIGNAL_TYPES=LINK_MODEL_BASED
/SIGNAL_NAMES=LumbarRateRot
/SIGNAL_FOLDER=ORIGINAL
/EVENT_NAME=MaxTorsoRot
!/SELECT_X=FALSE
!/SELECT_Y=FALSE
/SELECT_Z=TRUE
!/FRAME_WINDOW=8
/START_AT_EVENT=THLD1
/END_AT_EVENT=THLD2
/EVENT_INSTANCE=0
;
```

Calculates the time between the event sequence of the left heel marker, left toe marker and left heel marker and is known as the left heel strike

```
Metric_Time_Between_Events
/RESULT_METRIC_NAME=LHS_STRIDE
!/RESULT_METRIC_FOLDER=PROCESSED
/EVENT_SEQUENCE=LHS+LTO+LHS
/EXCLUDE_EVENTS=Thld1+Thld2
/GENERATE_MEAN_AND_STDDEV=FALSE
!/APPEND_TO_EXISTING_VALUES=FALSE
;
```

Appendix A (Continued)

Calculates the time between the event sequence of the right heel marker, right toe marker and right heel marker and is known as the right heel strike

```
Metric_Time_Between_Events
/RESULT_METRIC_NAME=RHS_STRIDE
!/RESULT_METRIC_FOLDER=PROCESSED
/EVENT_SEQUENCE=RHS+RTO+RHS
/EXCLUDE_EVENTS=Thld1+Thld2
/GENERATE_MEAN_AND_STDDEV=FALSE
!/APPEND_TO_EXISTING_VALUES=FALSE
;
```

Creates a table of time metrics from the event markers of the right heel strike marker

```
Evaluate_Expression
/EXPRESSION=1/METRIC::PROCESSED::RHS_STRIDE
/RESULT_NAME=RHS_CADENCE
!/RESULT_TYPE=DERIVED
!/RESULT_FOLDER=PROCESSED
;
```

Creates a table of time metrics from the event markers of the left heel strike marker

```
Evaluate_Expression
/EXPRESSION=1/METRIC::PROCESSED::LHS_STRIDE
/RESULT_NAME=LHS_CADENCE
!/RESULT_TYPE=DERIVED
!/RESULT_FOLDER=PROCESSED
;
```

Locates and creates a table of the amount of steps for the left heel strike marker and cadence is calculated from the events

```
Metric_Median
/RESULT_METRIC_NAME=LHS_CADENCE
!/APPLY_AS_SUFFIX_TO_SIGNAL_NAME=FALSE
/RESULT_METRIC_FOLDER=PROCESSED
/SIGNAL_TYPES=DERIVED
/SIGNAL_NAMES=LHS_CADENCE
/SIGNAL_FOLDER=PROCESSED
!/SIGNAL_COMPONENTS=ALL_COMPONENTS
/EVENT_SEQUENCE=
/EXCLUDE_EVENTS=
/GENERATE_MEAN_AND_STDDEV=FALSE
/APPEND_TO_EXISTING_VALUES=FALSE
;
```


Appendix A (Continued)

Locates and creates a table of the amount of steps for the right heel strike and cadence is calculated from the events

```
Metric_Median
/RESULT_METRIC_NAME=RHS_CADENCE
/APPLY_AS_SUFFIX_TO_SIGNAL_NAME=FALSE
/RESULT_METRIC_FOLDER=PROCESSED
/SIGNAL_TYPES=DERIVED
/SIGNAL_NAMES=RHS_CADENCE
/SIGNAL_FOLDER=PROCESSED
/SIGNAL_COMPONENTS=ALL_COMPONENTS
/EVENT_SEQUENCE=
/EXCLUDE_EVENTS=
/GENERATE_MEAN_AND_STDDEV=FALSE
/APPEND_TO_EXISTING_VALUES=FALSE
;
```

Applies a formula to the processed parameters of both left and right cadence numbers

```
Evaluate_Expression
/EXPRESSION=120*(METRIC::PROCESSED::LHS_CADENCE+METRIC::PROCESSED::RHS_CADENCE)/2
/RESULT_NAME=AVG_CADENCE
!/RESULT_TYPE=DERIVED
!/RESULT_FOLDER=PROCESSED
;
```

Calculates the distance between the event markers using the sequence of left heel marker, left toe marker and left heel marker for stride length of the left side

```
Metric_Vector_Between_Events
/RESULT_METRIC_NAME=TotalStrideL_Metric
!/RESULT_METRIC_FOLDER=PROCESSED
/GENERATE_VECTOR_LENGTH_METRIC=TRUE
/START_SIGNAL_TYPE=TARGET
/START_SIGNAL_NAME=LHEE
!/START_SIGNAL_FOLDER=ORIGINAL
/END_SIGNAL_TYPE=TARGET
/END_SIGNAL_NAME=LHEE
!/END_SIGNAL_FOLDER=ORIGINAL
/EVENT_SEQUENCE=LHS+LTO+LHS
/EXCLUDE_EVENTS=Thld1+Thld2
/GENERATE_MEAN_AND_STDDEV=FALSE
!/APPEND_TO_EXISTING_VALUES=FALSE
!/RETAIN_NO_DATA_VALUES=FALSE
;
```

Appendix A (Continued)

Calculates the distance between the event markers using the sequence of right heel marker, right toe marker and right heel marker for stride length of the right side

```
Metric_Vector_Between_Events
/RESULT_METRIC_NAME=TotalStrideR_Metric
!/RESULT_METRIC_FOLDER=PROCESSED
/GENERATE_VECTOR_LENGTH_METRIC=TRUE
/START_SIGNAL_TYPE=TARGET
/START_SIGNAL_NAME=RHEE
!/START_SIGNAL_FOLDER=ORIGINAL
/END_SIGNAL_TYPE=TARGET
/END_SIGNAL_NAME=RHEE
!/END_SIGNAL_FOLDER=ORIGINAL
/EVENT_SEQUENCE=RHS+RTO+RHS
/EXCLUDE_EVENTS=Thld1+Thld2
/GENERATE_MEAN_AND_STDDEV=FALSE
!/APPEND_TO_EXISTING_VALUES=FALSE
!/RETAIN_NO_DATA_VALUES=FALSE
;
```

Appendix B - APDM Release Statement

Simoes, Mario A.

From: matthew.monroe.johnson@gmail.com on behalf of Matthew Johnson [matt@apdm.com]
Sent: Friday, July 15, 2011 5:52 PM
To: Simoes, Mario A.
Subject: Re: Images and Papers
Attachments: APDM-ReleaseStatement.pdf

Mario,

Attached you will find the release statement. Since I am unable to print the document and sign it, please use the receipt of this email as my electronic signature.

Regards,

Matt

Matthew Johnson
Director of Sales & Marketing
APDM, Inc.
2828 SW Corbett Ave, Suite 130
Portland, Oregon 97201
Skype: matt-m-johnson
Direct: 503.446.4055

Visit our website at www.apdm.com

On Fri, Jul 15, 2011 at 3:22 PM, Simoes, Mario A. <msimoes@draper.com> wrote:

Matt,

I would like to make sure I have a statement from you in regards to the images and papers of the image. The papers I used to describe the monitors are Arash's. I just wanted to make sure its ok to use those images since they are part of the APDM system. Thank you! For my thesis I need to add that release statement. Thanks!!

Mario Simoes

Mechanical Engineering

[\(813\)465-5478](tel:(813)465-5478)

Draper Laboratory

3802 Spectrum Blvd Suite 201

1

Appendix B (Continued)

RELEASE STATEMENT

July 15, 2011

Matthew M. Johnson
Director of Sales and Marketing
APDM Inc.
2828 SW Corbett Ave, Suite 130
Portland, OR 97201

Dear Mario Simoes,

This letter is regarding the use of APDM Inc. branded images, technical papers, and papers referred by APDM Inc. in our software, Mobility Lab. We have looked over your thesis, and grant you permission to use all APDM Inc. specific images and papers found within your thesis.

Regards,

Matthew Johnson
Electronically signed